



HAL
open science

Discovery of the first Mycobacterium tuberculosis MabA (FabG1) inhibitors through a fragment-based screening

Léo Faion, Kamel Djaout, Rosangela Frita, Catalin Pintiala, Francois-Xavier Cantrelle, Martin Moune, Alexandre Vandeputte, Kevin Bourbiaux, Catherine Piveteau, Adrien Herledan, et al.

► To cite this version:

Léo Faion, Kamel Djaout, Rosangela Frita, Catalin Pintiala, Francois-Xavier Cantrelle, et al.. Discovery of the first Mycobacterium tuberculosis MabA (FabG1) inhibitors through a fragment-based screening. *European Journal of Medicinal Chemistry*, 2020, 200, pp.112440. 10.1016/j.ejmech.2020.112440 . hal-02988077

HAL Id: hal-02988077

<https://hal.science/hal-02988077>

Submitted on 4 Nov 2020

HAL is a multi-disciplinary open access archive for the deposit and dissemination of scientific research documents, whether they are published or not. The documents may come from teaching and research institutions in France or abroad, or from public or private research centers.

L'archive ouverte pluridisciplinaire **HAL**, est destinée au dépôt et à la diffusion de documents scientifiques de niveau recherche, publiés ou non, émanant des établissements d'enseignement et de recherche français ou étrangers, des laboratoires publics ou privés.

Discovery of the first *Mycobacterium tuberculosis* MabA (FabG1) inhibitors through a Fragment-based screening

Léo Faion^{1#}, Kamel Djaout^{2#}, Rosangela Frita², Catalin Pintiala¹, Francois-Xavier Cantrelle^{3,4}, Martin Moune², Alexandre Vandeputte², Kevin Bourbiaux¹, Catherine Piveteau¹, Adrien Herledan¹, Alexandre Biela¹, Florence Leroux¹, Laurent Kremer^{5,6}, Mickael Blaise⁵, Abdalkarim Tanina⁷, René Wintjens⁷, Xavier Hanoulle^{3,4}, Benoit Déprez¹, Nicolas Willand¹, Alain R. Baulard², Marion Flipo^{*,1}

These authors contributed equally to this work

*marion.flipo@univ-lille.fr

1. Univ. Lille, Inserm, Institut Pasteur de Lille, U1177 - Drugs and Molecules for living Systems, F-59000 Lille, France
2. Univ. Lille, CNRS, Inserm, CHU Lille, Institut Pasteur de Lille, U1019 - UMR 9017 - CIIL - Center for Infection and Immunity of Lille, F-59000 Lille, France
3. Univ. Lille, Inserm, CHU Lille, Institut Pasteur de Lille, U1167 - RID-AGE - Risk Factors and Molecular Determinants of Aging-Related Diseases, F-59000 Lille, France
4. CNRS, ERL9002 - Integrative Structural Biology, F-59000 Lille, France
5. Institut de Recherche en Infectiologie de Montpellier (IRIM), Université de Montpellier, CNRS UMR 9004, 34293 Montpellier, France
6. INSERM, Institut de Recherche en Infectiologie de Montpellier, Montpellier, France
7. Unité Microbiologie, Chimie Bioorganique et Macromoléculaire (CP206/04), département RD3, Faculté de Pharmacie, Université Libre de Bruxelles, B-1050 Brussels, Belgium

Abstract

Mycobacterium tuberculosis (*M.tb*), the etiologic agent of tuberculosis, remains the leading cause of death from a single infectious agent worldwide. The emergence of drug-resistant *M.tb* strains stresses the need for drugs acting on new targets. Mycolic acids are very long chain fatty acids playing an essential role in the architecture and permeability of the mycobacterial cell wall. Their biosynthesis involves two fatty acid synthase (FAS) systems. Among the four enzymes (MabA, HadAB/BC, InhA and KasA/B) of the FAS-II cycle, MabA (FabG1) remains the only one for which specific inhibitors have not been reported yet. The development of a new LC-MS/MS based enzymatic assay allowed the screening of a 1280 fragment-library and led to the discovery of the first small molecules that inhibit MabA activity. A fragment from the anthranilic acid series was optimized into more potent inhibitors and their binding to MabA was confirmed by ¹⁹F ligand-observed NMR experiments.

Keywords

MabA inhibitors; fragment; FabG1; tuberculosis; mycolic acid

1. Introduction

Tuberculosis (TB), a disease caused by the bacillus *Mycobacterium tuberculosis* (*M.tb*), remains a major cause of death worldwide.[1][2] In 2018, an estimated 10.0 million people became ill with TB and an estimated 1.45 million people died from the consequences of the disease (1.2 million deaths among HIV-negative people and 250 000 deaths among HIV-positive people). In addition, multidrug-resistant-TB (MDR-TB) is becoming a major threat. Drug-sensitive TB regimen has remained unchanged for 40 years [3,4] and only recently, three new chemical entities, namely bedaquiline [5], delamanid [6] and pretomanid [7], which are still in phase 3 clinical trials, have been approved for the treatment of MDR-TB. In this context, the search for new anti-TB agents acting on yet unexplored targets is thus warranted.

The mycobacterial cell wall is a complex structure composed of four major biomolecules: mycolic acids, arabinogalactan, lipoarabinomannan and peptidoglycan.[8,9] Mycolic acids are very long chain fatty acids, containing between 70 and 90 carbon atoms. They play an essential role in the architecture and permeability of the cell envelope and are essential for the survival of the bacteria.[10,11] The biosynthesis of mycolic acids involves two types of fatty acid synthase (FAS) systems. FAS-I cycle is a multi-functional enzyme complex, which synthesizes short-chain fatty acids (C_{16} - C_{18} and C_{24} - C_{26}).[12,13] These fatty acids can form the α -alkyl chain (C_{24}) found in mycolic acids or can be used as primer substrates for their subsequent elongation by the FAS-II cycle.[11] FAS-II system is not capable of *de novo* synthesis. This cycle is composed of four enzymes that act successively to elongate the acyl-CoA (C_{16} - C_{18}) generated by FAS-I and form the very long meromycolic acid chains (C_{42} - C_{62}).[14] Enzymatic modifications provide functional groups to the meromycolic chain like cyclopropane, keto and methoxy groups. The Claisen condensation of the modified meromycolic chain with the α -alkyl short chain (C_{24}), followed by a reduction, leads to α -alkyl- β -hydroxy-mycolic acids.[8,11]

FAS-II is initiated by a Claisen condensation of malonyl-ACP and palmitoyl-CoA catalyzed by the β -ketoacyl-ACP synthase FabH. The β -ketoacyl-ACP formed is then reduced by MabA (FabG1), a β -ketoacyl-ACP reductase NADPH-dependent, to produce β -hydroxyacyl-ACP. The enzymes HadAB/BC (β -hydroxyacyl-ACP dehydratases) catalyze the dehydration of the β -hydroxyacyl-ACP into *trans*-2-enoyl-ACP, which is then reduced by InhA (enoyl-ACP reductase NADH-dependent) to produce an acyl-ACP elongated by two carbons. The FAS-II cycle continues with a Claisen condensation of the acyl-ACP previously formed and malonyl-ACP, catalyzed by KasA/B (β -ketoacyl-ACP synthase). Several iterative cycles catalyzed by MabA, HadAB/BC, InhA and KasA/B lead to the production of elongated acyl chain (C_{42} - C_{62}).[8,14]

InhA [15], MabA [16], HadB [17] and KasA [18] have been shown to be essential for bacterial growth, strengthening their attractiveness as valuable chemotherapeutic targets.[19]

Several antibiotics target FAS-II. Indeed, InhA is inhibited by isoniazid as well as by two second-line drugs, ethionamide and prothionamide.[20–22] HadAB is inhibited by isoxyl and thiacetazone [23–25] and KasA/B are inhibited by thiolactomycin [26,27] while KasA (but not KasB) is also the target of an indazole sulfonamide (GSK3011724A).[28] However, no specific inhibitors of MabA have been reported yet.

The crystal structure of the *apo*-form MabA from *M.tb* was solved but several residues were not visible in the electron density.[29] A double mutant C60V/S144L of MabA was used to obtain crystal structures in the presence and absence of NADP. Nevertheless, in the *holo* form, the nicotinamide moiety and the ribose group were not visible in the electron density.[30] High-resolution crystal structures of MabA from *M. smegmatis* in its *apo*, NADP⁺-bound and NADPH-bound forms were recently reported.[31]

Structural comparison of MabA, a NADPH-dependent-ketoacyl-ACP reductase, and InhA, an NADH-dependent enoyl-ACP reductase, revealed the presence of hydrophobic substrate binding pockets of similar sizes.[29,32,33] However, MabA shares only 20% sequence identity with InhA or with other enoyl-ACP reductases, despite the similarity of their respective ligands. MabA has the same specificity for long-chain substrates as InhA. INH is a pro-drug which is bioactivated by the bacterial catalase peroxidase KatG to form an INH-NAD adduct that binds to and inhibits InhA. The interaction between MabA and the INH-NADP adduct has also been investigated and reported to lead to the inhibition of MabA activity *in vitro*. [34]

In order to discover the first drug-like MabA inhibitors, we developed a new LC-MS/MS-based enzymatic assay. To enhance the propensity to find inhibitors with physicochemical properties adequate to penetrate into mycobacteria, we used low-molecular-weight compounds, more properly called fragments, as a source of screening molecules.

2. Results and discussion

2.1 Development of LC-MS/MS based MabA activity assay

MabA is able to catalyze the reduction of acetoacetyl-CoA (AcAcCoA) into hydroxybutyryl-CoA (HBCoA) using NADPH as a cofactor (Figure 1A). An enzymatic assay based on the monitoring of the oxidation of NADPH by spectrophotometry was reported in the literature.[35,36] To develop an enzymatic assay suitable for high-throughput screening in 384-well plates, we chose to detect the formation of the enzymatic reaction product HBCoA by mass spectrometry. The enzymatic reaction was stopped by adding a solution of trifluoroacetic acid in water at a final concentration of 1%, containing butyryl-CoA (BCoA) as an internal standard for MS/MS analysis. The peak areas of HBCoA and BCoA were measured by MS/MS. To determine the initial velocity phase of the enzymatic reaction, we plotted the area of HBCoA peak as a function of reaction time from 2.5 to 20 min (Figure 1B). In view of this result, we opted to quench the reaction after 15 min in all the following experiments, which insures that the assay reflects the initial velocity phase of the reaction.[37]

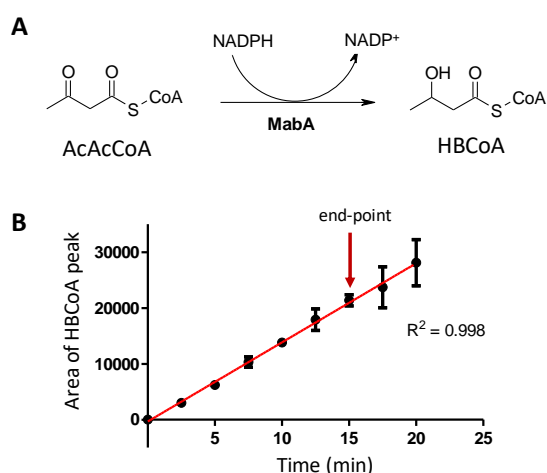


Figure 1. A. Reduction of AcAcCoA into HBCoA and oxidation of NADPH into NADP⁺ catalyzed by MabA. B. Progress curve of HBCoA formation as a function of enzymatic reaction time.

As mentioned above, the only MabA inhibitor reported so far in the literature is the adduct of INH with NADP⁺ (Figure 2A).[34] This INH-NADP adduct can be formed *in situ* using Mn^{III} [38] and was used as a reference inhibitor in this assay. LC-MS/MS measurement of HBCoA peak area in the absence (Figure 2B) or in the presence (Figure 2C) of this inhibitor allowed the calculation of a percentage of inhibition

and the determination of an IC_{50} . In this assay, the INH-NADP adduct displayed an IC_{50} of 20 μ M (Figure 2D). Triclosan [39] and pyridomycin [40,41], two known InHA inhibitors, did not show any MabA inhibitory activity in this assay when tested up to 100 μ M (data not shown).

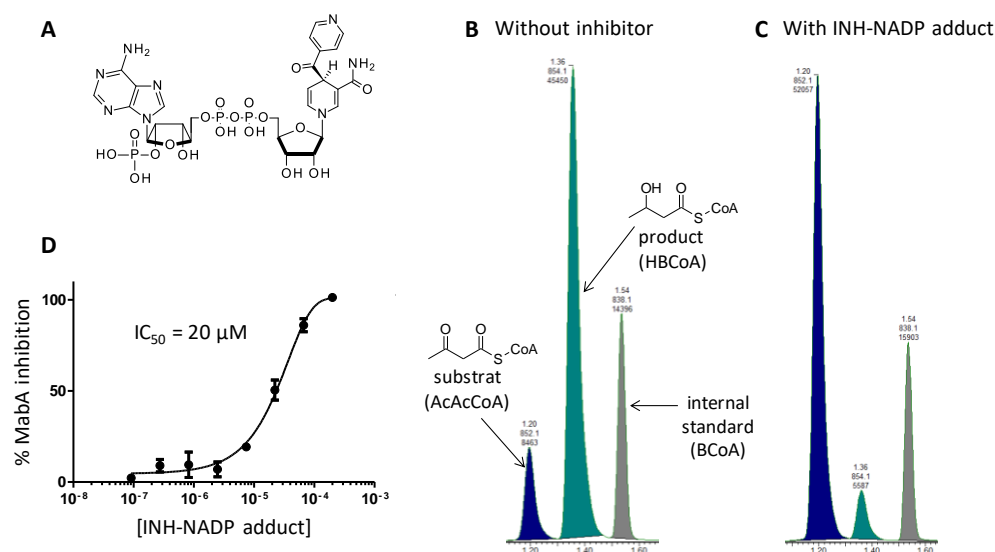


Figure 2. A. Structure of the INH-NADP adduct. B. Mass chromatogram obtained after 15 min of enzymatic reaction without inhibitor. C. Mass chromatogram obtained after 15 min of enzymatic reaction in the presence of INH-NADP adduct at 200 μ M. D. MabA inhibition with increasing doses of INH-NADP (curve was obtained using GraphPad Prism).

2.2 Screening

Our 1280-fragment library is composed of commercially available molecules and sp^3 and spiro-enriched compounds.[42,43] This library fulfills the ‘rule of three’ and all compounds are soluble in DMSO at 100 mM.[44] The 1280 fragments were screened at 1 mM on MabA at a concentration of 400 nM, using the mass spectrometry enzymatic assay adapted in 384-well plates. To identify both slow and fast binding inhibitors, fragments were incubated for 10 or 30 min with MabA alone in Hepes buffer. AcAcCoA and NADPH were then added to reach the final concentration of 50 μ M and the microplates were incubated 15 min at 22 °C. The reaction was stopped by the addition of a solution of trifluoroacetic acid in water containing BCoA. The peak areas of HBCoA and BCoA were measured by LC-MS/MS. To confirm the statistical validity of the screening, Z' -factors were calculated using the mean and standard deviation values of the negative (1% DMSO) and positive controls (INH-NADP adduct at 200 μ M). All the screening plates displayed a Z' -factor between 0.72 and 0.83. It is frequently admitted that a Z' -factor ≥ 0.5 is acceptable for high-throughput screening.[45][46]

Percentage of inhibition of each compound was calculated using the mean values of the negative and positive controls (Figure 3). Similar inhibition percentages were obtained for the two incubation conditions, suggesting that compounds are more likely fast binding inhibitors. Fifty compounds displaying an inhibition percentage greater than 30% were selected for dose response experiments, which allowed to identify 12 fragments with IC_{50} lower than 300 μ M. Data mining of commercial libraries identified 68 analogues of these 12 fragments. Retesting of the 80 compounds in dose-response experiments led to the selection of 6 chemical series displaying IC_{50} s ranging from 25 to 300 μ M (Figure 4).

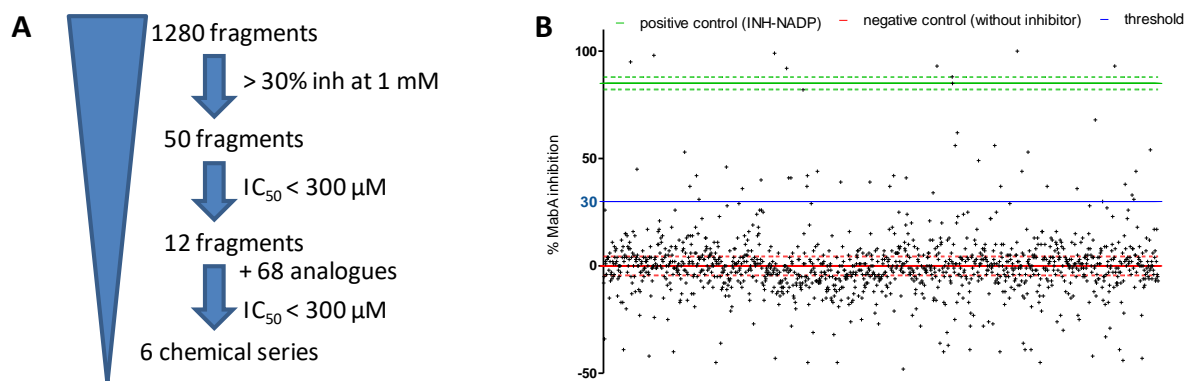


Figure 3. A. Screening cascade. B. Screening result of fragments incubated 30 min with MabA before the initiation of the enzymatic reaction. Black crosses: percentage of inhibition of each fragment. Green: median values and standard deviations of the positive control (INH-NADP adduct at 200 μM). Red: median values and standard deviations of the negative control (1% DMSO). Blue: threshold at 30% of inhibition.

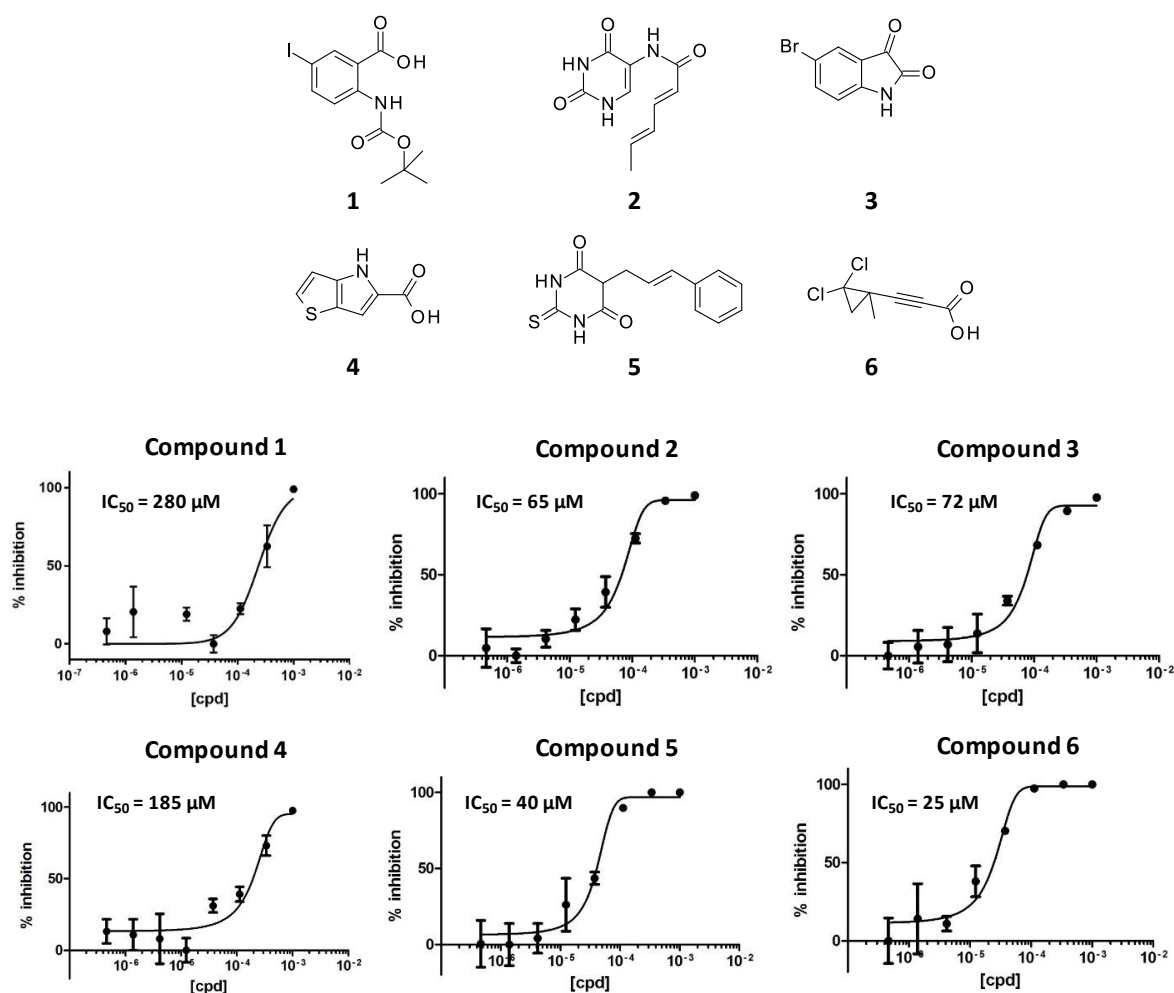


Figure 4. Structures and DRCs of one hit in each chemical series identified during the screening.

2.3 Selection of a chemical series

An early structure-activity relationships (SAR) study was initiated on each of the six series. Briefly, whereas compound **1** of the anthranilic acid series was retested three times in duplicate and displayed an IC₅₀ slightly higher than that obtained during the screening ($430 \pm 26 \mu\text{M}$), the early SAR in this series

led to compounds with improved activities that will be detailed later in this manuscript. In the 5-aminouracil series (compound **2**), the replacement of the pentadiene chain with other aliphatic chains led to inactive compounds ($IC_{50} > 1$ mM). For the isatine series, early SAR showed that the bromine atom of compound **3** can be removed or replaced by a fluorine atom, a chlorine atom or a methoxy group. In contrast, the 5-bromoindolin-2-one was shown inactive ($IC_{50} > 1$ mM) indicating that the ketone function is necessary for activity. Replacement of the thienopyrrole moiety of compound **4** with other fused aromatic rings was not tolerated ($IC_{50} > 1$ mM). In the thiobarbituric acid series (compound **5**), the substitution of the phenyl ring is tolerated and the replacement of the sulphur atom of the thiobarbituric core with an oxygen atom decreased the activity. Finally, in the propanoic acid series, the resynthesis of compound **6** led to an inactive compound ($IC_{50} > 1$ mM) whereas the commercial batch was reconfirmed as active as during the screening ($IC_{50} = 30$ μ M). This implies that the commercial product may not be the one described, although LC-MS analysis showed that it is relatively pure and that the mass is consistent with the described structure. Limited by the amount, we were unable to investigate further the structure of this compound that is no longer commercially available. The 6 hits were then tested on *M.tb*. Compounds **2-6** did not display antibacterial activity ($MIC_{90} > 300$ μ M) whereas compound **1** showed bacterial growth inhibition with a MIC_{90} of 300 μ M. Anthranilic acid represents a well-known privileged structure and its derivatives have been widely used in different fields of medicinal chemistry.[47–50] Nevertheless, compound **1** has not yet been described in the ChEMBL database as having any biological activities. This motivated us to further optimized this scaffold.

2.4 Competition with NADPH

In order to determine whether compound **1** acts as a competitive inhibitor of NADPH, the previously described HBCoA enzymatic assay was used in the presence of two different NADPH concentrations (50 and 500 μ M). This test was validated using the INH-NADP adduct in a dose-response experiment (Figure 5A). As expected, since the adduct is assumed to bind to the NADPH binding site, its IC_{50} was shifted towards highest concentrations in the presence of the high dose of NADPH ($IC_{50} = 61$ μ M when competing with 500 μ M of NADPH vs $IC_{50} = 20.3 \pm 0.6$ μ M (3 independent experiments) when competing with 50 μ M of NADPH). In contrast, in this assay compound **1** displays a similar IC_{50} whatever the concentration of NADPH used, suggesting that this compound inhibits MabA in a non-competitive manner with NADPH (Figure 5B). This compound could therefore interact with the substrate binding pocket, as it has been reported for InhA inhibitors that have been co-crystallized with their target. Indeed, most of these compounds occupy the lipid-binding pocket of InhA facing the nicotinamide moiety of NAD.[51–54]

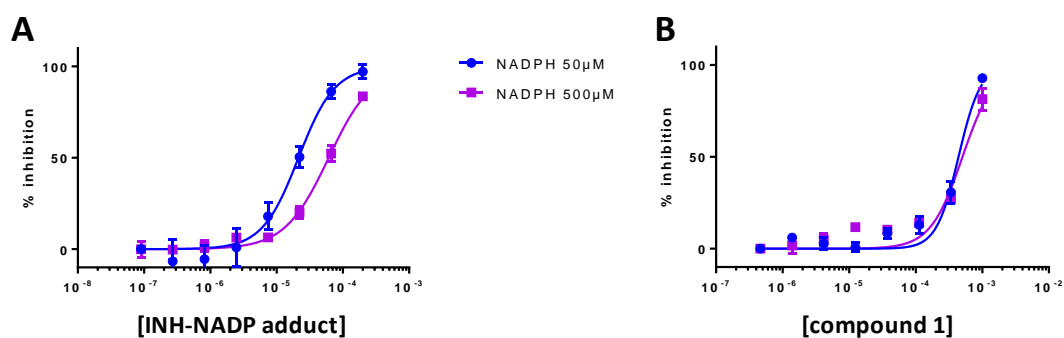


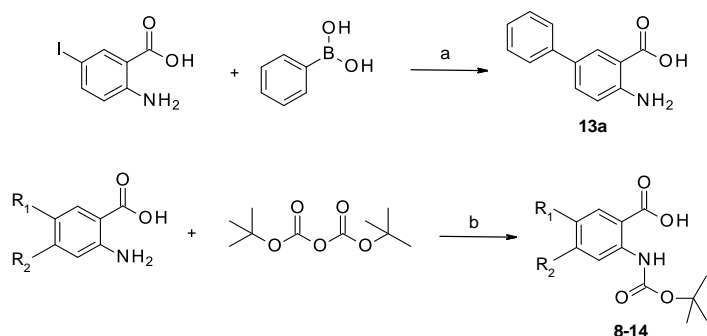
Figure 5. DRC of INH-NADP adduct (A) and compound 1 (B) with 50 and 500 μ M of NADPH.

2.5 Chemistry

In order to explore the SAR in the anthranilic acid series, the iodine atom, the Boc group and the carbamate function of compound **1** were modified.

2.5.1. Modifications of the substituents on the phenyl ring

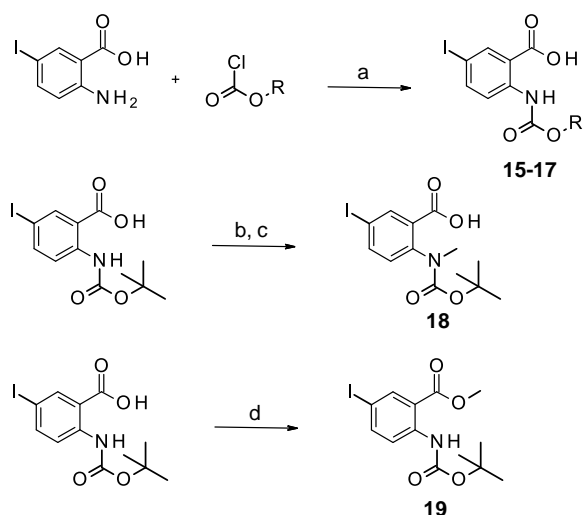
First, the importance of the iodine atom was evaluated by removing (compound **7**) or replacing it by other halogen atoms (compounds **8**, **9**, **10**). The iodine atom was also replaced by a methoxy group (compound **11**) or aromatic rings such as phenoxy (compound **12**) and phenyl groups (compound **13**). A naphthyl group (compound **14**) was also introduced instead of the 5-iodophenyl group to evaluate the impact of the substitution by an aromatic ring. Compound **7** was commercially available and compounds **8**, **9**, **10** were synthesized in one step from the 5-halogenoanthranilic acid and di-*tert*-butyldicarbonate (Boc₂O) in acetonitrile under microwave irradiations (Scheme 1). Compounds **11**, **12** and **14** were synthesized according to scheme 1 in pyridine at 90 °C. The 2-amino-5-phenylbenzoic acid was not commercially available and was synthesized in one step using a Suzuki coupling (Scheme 1). These intermediate **13a** was then reacted with Boc₂O in acetonitrile under microwave irradiations.



Scheme 1. Synthesis of Boc-2-aminobenzoic acid 8-14. Reagents and conditions: (a) PhB(OH)₂ (1 eq.), K₂CO₃ (2 eq), Pd/C (0.03 eq), H₂O, reflux, 4h. (b) Boc₂O (1.1 eq), DMAP (0.065 eq), TEA (1 eq), MeCN, μ W 40 °C, 15 min or Boc₂O (1.6 eq), pyridine, 90 °C, 2h30.

2.5.2. Modifications of the carbamate group and the carboxylic acid

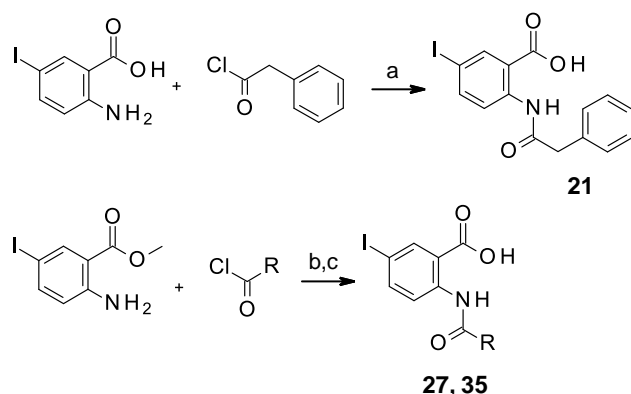
Replacement of the Boc group with other carbamate groups was evaluated and the carboxylic acid was replaced by a methyl ester. Carbamates (compounds **15-17**) were synthesized in one step from 2-amino-5-iodobenzoic acid and corresponding chloroformates in pyridine (Scheme 2). Compound **18** was obtained by methylation of the nitrogen atom using iodomethane. This led also to the formation of the methyl ester that was hydrolyzed in basic conditions. The methyl ester (compound **19**) was obtained by reaction of the carboxylic acid with dimethylsulfate using potassium carbonate as base.



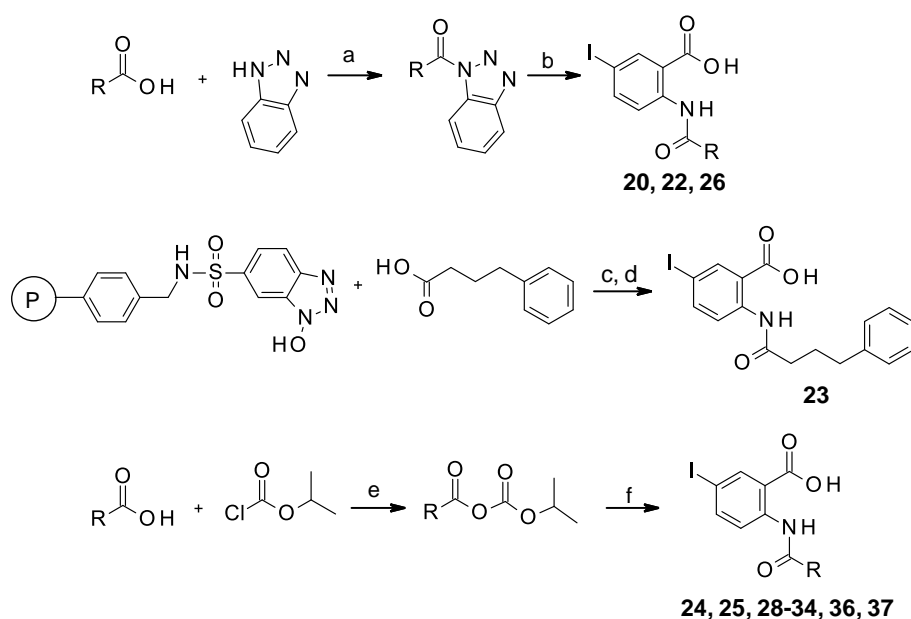
Scheme 2. Synthesis of compounds 15-19. Reagents and conditions: (a) 2-amino-5-iodobenzoic acid (1 eq), chloroformate (2 eq), anh. pyridine, RT, 1-2h; (b) iodomethane (4.6 eq), Cs₂CO₃ (7 eq), anh. DMF, RT, 48 h; (c) NaOH (7 eq), MeOH, H₂O, RT, 2 days; (d) dimethylsulfate (2 eq), K₂CO₃ (2 eq), MeCN, RT, 2h.

2.5.3. Replacement of the carbamate with an amide

The carbamate function was then replaced by an amide function variously substituted (compounds **20-37**). Several methods were attempted for the coupling of the amine function of the 2-amino-5-iodobenzoic acid with diverse acyl chlorides (Scheme 4) or carboxylic acids (Scheme 4). Acyl chlorides were coupled directly with 2-amino-5-iodobenzoic acid in pyridine (compound **21**) or with methyl 2-amino-5-iodobenzoate and then the methyl ester was hydrolyzed in basic conditions (compounds **27** and **35**). Carboxylic acids were activated either by reaction with thionyl chloride and 1H-benzotriazole (compounds **20**, **22**, and **26**), by using an HOBt-resin [55] (compound **23**) or by forming a mixed anhydride with isopropyl chloroformate (compounds **24**, **25**, **28-34** and **36-37**). All these reactions led to the desired analog with moderate yields (~50%) after reverse chromatography purification. We found that the most appropriate way to activate carboxylic acids for the coupling with 2-amino-5-iodobenzoic acid was through the synthesis of mixed anhydrides using isopropyl chloroformate.



Scheme 3. Synthesis of compounds 21, 27 and 35 from acyl chlorides. Reagents and conditions: (a) 2-amino-5-iodo-benzoic acid (1 eq), 2-phenylacetyl chloride (2.5 eq), anh. pyridine, RT, 2h; (b) methyl 2-amino-5-iodo-benzoate (1 eq), acyl chloride (1.1 eq), anh. pyridine, RT, 2h. (c) LiOH (3 eq), H₂O, THF, RT, 1h.



Scheme 4. Synthesis of compounds 20, 22-26, 28-34 and 36-37 from carboxylic acids. Reagents and conditions: (a) SOCl_2 (1.1 eq), 1H-benzotriazole (3.1 eq), carboxylic acid (1 eq), DCM, RT, overnight; (b) 2-amino-5-iodo-benzoic acid (1 eq), DMAP (1.1 eq), CHCl_3 , μW 80 °C, 15-30 min; (c) 4-phenylbutanoic acid (3 eq), PyBrop (3 eq), DIEA (6 eq), HOBt resin (1 eq), DMF, RT, 3h; (d) 2-amino-5-iodo-benzoic acid (0.8 eq), DMF, RT, overnight; (e) isopropyl chloroformate 1 M in toluene (1.5 eq), carboxylic acid (1eq), TEA (1.2 eq), anh. THF, RT, overnight; (f) 2-amino-5-iodo-benzoic acid (0.67 eq), Na_2CO_3 (1.33 eq), THF, H_2O , RT, 3h to overnight.

2.6 Biological results

All compounds were evaluated for their inhibitory activity of MabA using our HBCoA enzymatic assay. Activities are reported in comparison to the inhibitory activity of compound **1**.

2.6.1. Modifications of the substituents on the phenyl ring

Cpd	R1	R2	% inh ^a	IC ₅₀ (μM)
1	I	H	100	430 ± 26
7	H	H	31	> 1000
8	F	H	38	470
9	Cl	H	77	> 500
10	Br	H	95	470
11	OCH ₃	H	31	> 1000
12	OPh	H	100	243
13	Ph	H	100	194
14			100	310

Table 1. Biological activities of compounds **1**, **7-14**. ^a Percentage of inhibition (compounds tested at 1 mM)

Replacement of the iodine atom with other halogen atoms (compounds **8-10**) led to a decrease in activity related to the size of the atom. Indeed, compound **8** bearing a fluorine atom in position 5 displayed the lowest activity while compound **10** bearing a bromine atom was slightly less active than the reference compound **1**. Moreover, replacement of the iodine atom with a hydrogen atom (compound **7**) was detrimental for activity ($IC_{50} > 1$ mM). Introduction of a methoxy group (compound **11**) led to an inactive compound whereas introduction of hydrophobic groups like phenoxy or phenyl (compounds **12** and **13**) increased activity twice. Interestingly, a naphthyl ring (compound **14**) instead of the 5-iodophenyl was also tolerated. These first SAR showed that replacement of the iodine atom with an aromatic ring had a favorable impact on activity.

2.6.2. Modifications of the carbamate and the carboxylic acid

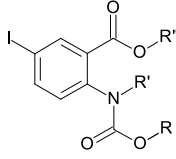
					
Cpd	R	R'	R''	% inh ^a	IC ₅₀ (μM)
1	tBu	H	H	100	430 ± 26
15	iBu	H	H	100	310
16	allyl	H	H	83	> 500
17	CH ₂ -Ph	H	H	100	92 ± 3.5
18	tBu	CH ₃	H	50	~ 1000
19	tBu	H	CH ₃	0	> 1000

Table 2. Biological activities of compounds **1**, **15-19**. ^a Percentage of inhibition (compounds tested at 1 mM)

In the carbamate series, replacement of the tertbutyl group with an isobutyl group (compound **15**) led to a compound with a similar activity ($IC_{50} = 310$ μM). Replacement with an allyl group (compound **16**) led to a less active compound ($IC_{50} > 500$ μM) whereas introduction of a benzyl group (compound **17**) provided a 4-fold increase in potency ($IC_{50} = 92$ μM). Methylation of the carbamate (compound **18**) or replacement of the carboxylic acid with a methyl ester (compound **19**) was detrimental for activity ($IC_{50} > 1000$ μM).

2.6.3. Replacement of the carbamate with an amide

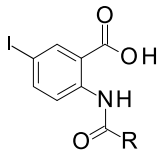
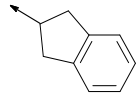
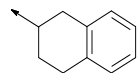
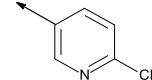
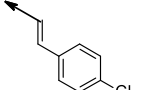
					
Cpd	R	IC ₅₀ (μM)	Cpd	R	IC ₅₀ (μM)
20	Ph	145	29	3,4-Cl ₂ -Ph	38 ± 6
21	CH ₂ -Ph	> 500	30	2,4-Cl ₂ -Ph	126
22	(CH ₂) ₂ -Ph	295	31	4-CH ₃ -Ph	95
23	(CH ₂) ₃ -Ph	186	32	4-CF ₃ -Ph	69
24		140	33	4-OCF ₃ -Ph	84
25		109	34	3-CF ₃ -4-Cl-Ph	59
26	cyclopropyl	> 500	35	4-pyridyl	> 400
27	3-Cl-Ph	70	36		147
28	4-Cl-Ph	53	37		40

Table 3. Biological activities of compounds 20-36.

To further enhance the potency and explore the SAR, we examined the effect of changing the carbamate function with an amide function. Introduction of aliphatic chains like methyl, *tert*-butyl or neopentyl was not tolerated (data not shown) while compound **20** bearing a phenyl ring displayed an IC₅₀ of 145 μM. Interestingly, the chain length between the amide function and the phenyl ring seemed important for activity. Indeed, introduction of one, two or three methylene groups (compounds **21-23**) led to a decrease in activity (IC₅₀ > 500 μM, 295 and 186 μM, respectively) compared to compound **20**, whereas a more constrained linker, like a cyclopentyl (compound **24**) or a cyclohexyl (compound **25**), restored activity. Replacement of the phenyl ring with an aliphatic ring like a cyclopropyl (compound **26**) proved detrimental (IC₅₀ > 500 μM). Compound **20** bearing a phenyl group directly connected to the amide function displaying the best activity, the phenyl ring was then substituted in different positions. Introduction of a chlorine atom in meta or para position (compounds **27** and **28**) was favorable for activity (IC₅₀ = 70 μM and 53, respectively) whereas introduction of electron donating or withdrawing groups like a methyl, a trifluoromethyl or a trifluoromethoxy group (compounds **31-33**) slightly decreased activity. Keeping the chlorine atom in para position, we introduced an unsaturated chain between the amide function and the phenyl ring that led to a modest increase of activity (compound **37** IC₅₀ = 40 μM). Introduction of an additional chlorine atom in position 2 of the phenyl ring (compound **30** IC₅₀ = 126 μM) led to a compound three times less active than compound **29** bearing a second chlorine atom in position 3 (IC₅₀ = 38 ± 6 μM), suggesting that position 2 may be

sensitive to steric hindrance. Replacement of the chlorine atom in position 3 of compound **29** with a trifluoromethyl group (compound **34**) led to a compound with a similar activity.

Finally, introduction of a pyridine ring proved detrimental for activity. Indeed, replacement of the phenyl ring (compound **20**) with a pyridine (compound **35**) was not tolerated ($IC_{50} > 400 \mu M$) and introduction of a nitrogen atom in the 4-chlorophenyl ring led to compound **36**, three times less active than compound **28** ($IC_{50} = 147 \mu M$ vs $IC_{50} = 53 \mu M$).

These SAR showed that the carbamate function could be replaced with an amide function and a phenyl ring proved optimal for activity. This led to the identification of compound **29** bearing a 3,4-dichlorophenyl ring on the amide function ($IC_{50} = 38 \pm 6 \mu M$).

2.6.4. Evaluation of the interaction of the fluorinated compounds with MabA by NMR

^{19}F ligand-observed NMR has been described as a powerful tool in detecting weak binding of small molecules. ^{19}F has a wide chemical shift range, therefore even small changes in binding can result in a measurable shift in the fluorine signal.[56,57] Such experiments were conducted to confirm the binding of the fluorinated inhibitors to the targeted protein MabA. Three compounds (**32-34**) bearing a trifluoromethyl group were selected and NMR experiments were performed using a 600 MHz spectrometer equipped with a ^{19}F cryogenic probe. The perturbations (broadening and chemical shift changes) of ^{19}F -NMR signal of the three compounds in the presence of MabA confirmed the direct binding of these inhibitors to the protein (Figure 6). Moreover, the quantification of the ^{19}F signal perturbations (area under the red curve) in this experiment allowed to rank the compounds according to their affinity for MabA. Remarkably, the three compounds displayed a similar ranking in the NMR experiment and in the MabA enzymatic assay. The most significant ^{19}F -NMR-signal decrease was observed with compound **34** and among the three inhibitors this compound showed a slightly better inhibitory activity ($IC_{50} = 59 \mu M$ vs 69 and 84 μM).

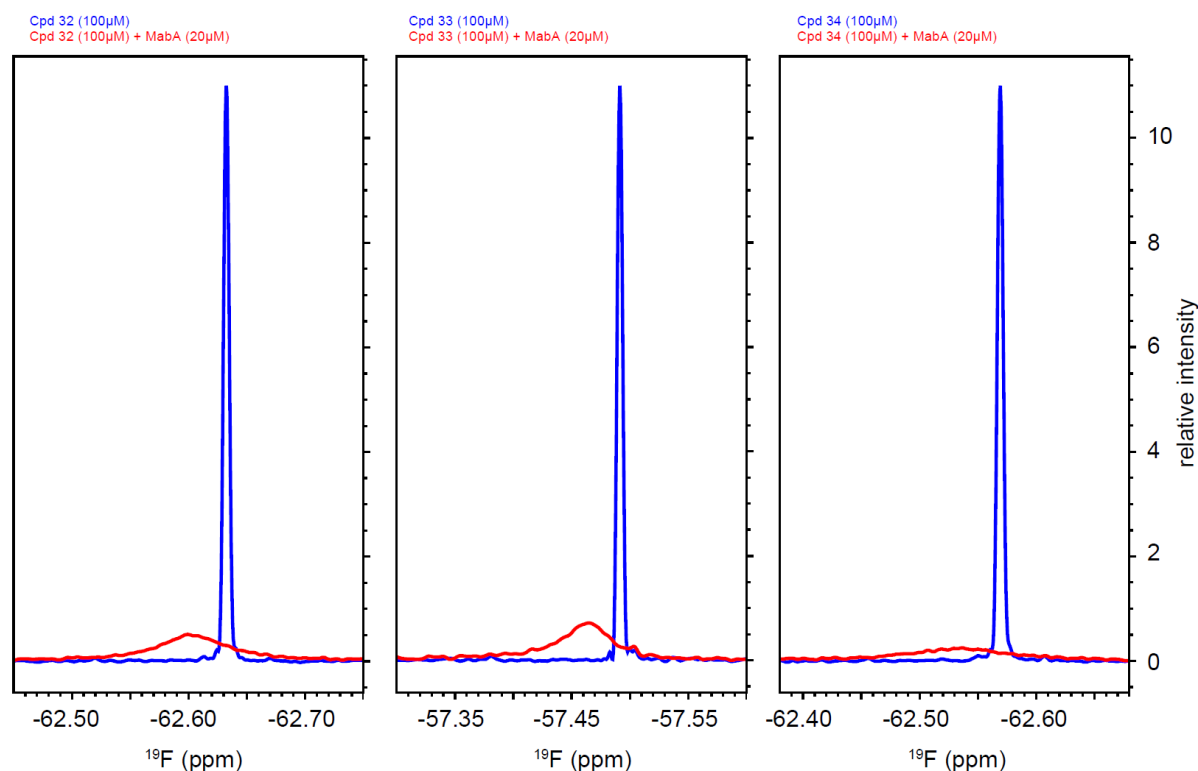


Figure 6. 1D ^{19}F NMR spectra of compounds **32-34** at 100 μM alone (blue signal) and in the presence of MabA at 20 μM (red signal).

2.6.5. Evaluation of physico-chemical properties and assessment of antimycobacterial activity

The physico-chemical properties of the most active compound (compound **29**) were measured. This compound displayed a solubility greater than 200 μM and a logD equal to 3.40. Compound **29** was then tested on *M.tb* grown in Middlebrook 7H9 liquid medium (pH 6.6). Despite the 10 fold-improved inhibitory activity of compound **29** compared to compound **1** in the MabA enzymatic inhibitory assay, both compounds showed the same bacterial growth inhibition ($\text{MIC}_{90} = 300 \mu\text{M}$, which corresponds to 130 and 110 $\mu\text{g}/\text{mL}$ respectively). The antimicrobial activity of carboxylic acids, such as benzoic acid, salicylic acid, aspirin (acetyl-salicylic acid) or mefenamic acid (an anthranilic acid derivative) have been reported in the literature.[58] These weak acids displayed MIC between 33 and 111 $\mu\text{g}/\text{mL}$ in culture medium at pH 6.8 and have been proposed, by Zhang et al., to act by disrupting the membrane potential of the bacteria. At this stage, our data do not allow to conclude formally that the antimicrobial activity observed for compound **29** is exclusively due to MabA inhibition. Mechanism of action similar to the one hypothesized for related carboxylic acids has also to be considered. Optimization of compound **29** is in progress and further experiments will be conducted to clarify this point.

3. Conclusion

A new LC-MS/MS based MabA activity assay was developed and used for the screening of a 1280-fragment library. This allowed identification of the first specific inhibitors of MabA, an essential enzyme involved in *M.tb* mycolic acid biosynthesis. From the 6 different chemical series validated by dose-response experiments, the anthranilic acid series was chosen for structure-activity relationships studies and we were able to define the essential molecular features that governs MabA inhibition. ^{19}F ligand-observed NMR experiments confirmed the binding of three fluorinated analogues of this series to MabA. The most potent inhibitor, bearing a 3,4-dichlorophenyl ring on the amide function (compound **29**), inhibited MabA with an IC_{50} of 38 μM and bacterial growth with a MIC_{90} of 300 μM . Optimization in this series of compounds will be pursued in order to increase their affinity to MabA as well as their ability to inhibit *M.tb* growth. This optimization will help to clarify the mechanism of action of these compounds in bacteria. These results will be reported in due course.

4. Experimental section

4.1. Chemistry

Solvents for synthesis, analysis and purification were purchased as analytical grade from commercial suppliers and used directly without further purification. Chemical reagents were purchased from Fisher scientific, Merck, Fluorochem, Enamine or TCI as reagent grade and used without further purification. LC-MS Waters system was equipped with a 2747 sample manager, a 2695 separations module, a 2996 photodiode array detector (200-400 nm) and a Micromass ZQ2000 detector (scan 100-800). XBridge C18 column (50 mm x 4.6 mm, 3.5 μ m, Waters) was used. The injection volume was 20 μ L. A mixture of water and acetonitrile was used as mobile phase in gradient-elution. The pH of the mobile phase was adjusted with HCOOH and NH₄OH to form a buffer solution at pH 3.8. The analysis time was 5 min (at a flow rate at 2 mL/min), 10 min (at a flow rate at 1 mL/min) or 30 min (at a flow rate at 1 mL/min). Purity (%) was determined by reversed phase HPLC, using UV detection (215 nm), and all isolated compounds showed purity greater than 95%.

HRMS analysis was performed on a LC-MS system equipped with a LCT Premier XE mass spectrometer (Waters), using a XBridge C18 column (50 mm x 4.6 mm, 3.5 μ m, Waters). A gradient starting from 98% H₂O 5 mM Ammonium Formate pH 3.8 and reaching 100% CH₃CN 5 mM Ammonium Formate pH 3.8 within 3 min at a flow rate of 1 mL/min was used.

NMR spectra were recorded on a Bruker DRX-300 spectrometer. The results were calibrated to signals from the solvent as an internal reference [e.g. 2.50 (residual DMSO-d₆) and 39.52 (DMSO-d₆) ppm for ¹H and ¹³C NMR spectra respectively]. Chemical shifts (δ) are in parts per million (ppm) downfield from tetramethylsilane (TMS). The assignments were made using one-dimensional (1D) ¹H and ¹³C spectra and two-dimensional (2D) HSQC-DEPT, COSY and HMBC spectra. NMR coupling constants (J) are reported in Hertz (Hz), and splitting patterns are indicated as follows: s for singlet, brs for broad singlet, d for doublet, t for triplet, q for quartet, quin for quintet, dd for doublet of doublet, ddd for doublet of doublet of doublet, dt for doublet of triplet, qd for quartet of doublet, m for multiplet, δ for chemical shift, J for coupling constant.

Reverse flash chromatography was performed using a CombiFlash[®] C₁₈ Rf200 with C₁₈ silica gel cartridges. UV detection (215 and 254 nm) was used to collect the desired product.

Preparative HPLC was performed using a Varian PROStar system with an OmniSphere 10 μ m column C₁₈ Dynamax (250 mm x 41.4 mm) from Agilent Technologies. A gradient starting from 20% MeCN / 80% H₂O / 0.1% formic acid and reaching 100% MeCN / 0.1% formic acid at a flow rate of 80 mL/min was used. UV detection (215 and 254 nm) was used to collect the desired product.

Syntheses under microwave irradiations were performed using Biotage[®] Initiator+.

4.1.1. General method for the synthesis of compounds **8**, **9** and **10**

2-amino-5-halogeno-benzoic acid (1 eq), di-*tert*-butyl dicarbonate (1.1 eq), DMAP (0.065 eq) and TEA (1 eq) were dissolved in MeCN (C = 0.9 M). The mixture was vortexed, heated at 40 °C under microwave irradiation for 15 min. The mixture was then filtrated through cotton. The filtrate was concentrated in vacuo and the residue was purified by preparative HPLC to give the desired product.

4.1.1.1. 2-(*tert*-butoxycarbonylamino)-5-fluoro-benzoic acid (**8**)

Yield: 45%. ¹H-NMR (DMSO-d₆): δ (ppm) 13.93 (brs, OH), 10.33 (s, NH), 8.27 (dd, J = 9.3 Hz, J = 5.1 Hz, 1H), 7.66 (dd, J = 9.4 Hz, J = 3.1 Hz, 1H), 7.46 (ddd, J = 9.3 Hz, J = 7.9 Hz, J = 3.1 Hz, 1H), 1.48 (s, 9H). ¹³C-NMR (DMSO-d₆): δ (ppm) 168.9 (d, J = 2.4 Hz), 156.5 (d, J = 239.4 Hz), 152.6, 138.4 (d, J = 2.1 Hz), 121.6 (d, J = 21.7 Hz), 120.7 (d, J = 7.1 Hz), 117.4, 117.2 (d, J = 23.8 Hz), 28.4. HRMS (TOF, ES-) m/z [M-H]⁻ calculated for C₁₂H₁₃NO₄F 254.0829, found 254.0835.

4.1.1.2. 2-(tert-butoxycarbonylamino)-5-chloro-benzoic acid (9)

Yield: 45%. ¹H-NMR (DMSO-d₆): δ (ppm) 14.0 (brs, OH), 10.5 (s, NH), 8.30 (d, *J* = 9.0 Hz, 1H), 7.90 (d, *J* = 2.6 Hz, 1H), 7.63 (dd, *J* = 9.0 Hz, *J* = 2.7 Hz, 1H), 1.48 (s, 9H). ¹³C-NMR (DMSO-d₆): δ (ppm) 168.9, 152.3, 140.8, 134.3, 130.7, 125.5, 120.5, 117.5, 81.0, 28.3. HRMS (TOF, ES-) *m/z* [M-H]⁻ calculated for C₁₂H₁₃NO₄Cl 270.0533, found 270.0553.

4.1.1.3. 5-bromo-2-(tert-butoxycarbonylamino)benzoic acid (10)

Yield: 28%. ¹H-NMR (DMSO-d₆): δ (ppm) 13.99 (brs, OH), 10.45 (s, NH), 8.26 (d, *J* = 9.0 Hz, 1H), 8.02 (d, *J* = 2.5 Hz, 1H), 7.75 (dd, *J* = 9.0 Hz, *J* = 2.5 Hz, 1H), 1.48 (s, 9H). ¹³C-NMR (DMSO-d₆): δ (ppm) 168.8, 152.3, 141.2, 137.1, 133.6, 120.7, 117.7, 113.2, 81.0, 28.3. HRMS (TOF, ES-) *m/z* [M-H]⁻ calculated for C₁₂H₁₃NO₄Br 314.0028, found 314.0040.

4.1.2. General method for the synthesis of compounds 11, 12 and 14

Di-*tert*-butyl dicarbonate (Boc₂O) (1.1 eq) was added to a solution of the appropriate amine (1 eq) dissolved in anhydrous pyridine (C = 1 M). The mixture was stirred at 90 °C for 1h30, then Boc₂O (0.5 eq) was added and the mixture was stirred at 90 °C for 1h. The reaction mixture was quenched with aqueous saturated NH₄Cl, the product was then extracted with EtOAc (3 times) and washed twice with aqueous saturated NH₄Cl, and then once with brine. The organic layer was dried over MgSO₄ and concentrated in vacuo. The residue was purified by preparative HPLC to give the desired product.

4.1.2.1. 2-(tert-butoxycarbonylamino)-5-methoxy-benzoic acid (11)

Yield: 78%. ¹H-NMR (DMSO-d₆): δ (ppm) 10.22 (s, NH), 8.17 (d, *J* = 9.0 Hz, 1H), 7.43 (d, *J* = 3.0 Hz, 1H), 7.19 (dd, *J* = 9.1 Hz, *J* = 3.1 Hz, 1H), 3.75 (s, 3H), 1.47 (s, 9H). ¹³C-NMR (DMSO-d₆): δ (ppm) 169.7, 153.8, 152.7, 135.3, 121.0, 120.4, 117.2, 115.1, 80.2, 55.8, 28.4. HRMS (TOF, ES-) *m/z* [M-H]⁻ calculated for C₁₃H₁₆NO₅ 266.1028, found 266.1038.

4.1.2.2. 2-(tert-butoxycarbonylamino)-5-phenoxy-benzoic acid (12)

Yield: 36%. ¹H-NMR (DMSO-d₆): δ (ppm): 13.71 (brs, OH), 10.34 (s, NH), 8.29 (d, *J* = 9.2 Hz, 1H), 7.50 (d, *J* = 3.0 Hz, 1H), 7.39 (tt, *J* = 8.58 Hz, *J* = 7.4 Hz, *J* = 2.1 Hz, 2H), 7.32 (dd, *J* = 9.1 Hz, *J* = 3.0 Hz, 1H), 7.14 (tt, *J* = 7.38, 1.1 Hz, 1H), 7.00 (dd, *J* = 8.58, 1.0 Hz, 2H), 1.48 (s, 9H). ¹³C-NMR (DMSO-d₆): δ (ppm): 168.8, 156.9, 152.1, 150.1, 137.4, 130.1, 125.3, 123.4, 120.6, 120.2, 118.2, 116.8, 80.1, 27.9. HRMS (TOF, ES-) *m/z* [M-H]⁻ calculated for C₁₈H₁₈NO₅ 328.1185, found 328.1197.

4.1.2.3. 3-(tert-butoxycarbonylamino)naphthalene-2-carboxylic acid (14)

Yield: 42%. ¹H-NMR (DMSO-d₆): δ (ppm) 13.83 (brs, OH), 10.51 (s, NH), 8.68 (d, *J* = 5.7 Hz, 2H), 8.01 (d, *J* = 7.6 Hz, 1H), 7.85 (d, *J* = 7.7 Hz, 1H), 7.59 (dd, *J* = 7.0 Hz, *J* = 1.2 Hz, 1H), 7.44 (dd, *J* = 7.0 Hz, *J* = 1.2 Hz, 1H), 1.52 (s, 9H). ¹³C-NMR (DMSO-d₆): δ (ppm) 169.6, 152.2, 136.7, 135.8, 133.3, 129.3, 129.1, 127.5, 126.8, 125.1, 116.5, 114.3, 80.0, 28.0. HRMS (TOF, ES-) *m/z* [M-H]⁻ calculated for C₁₆H₁₆N O₄ 286.1079, found 286.1104.

4.1.3. 2-(tert-butoxycarbonylamino)-5-phenyl-benzoic acid (13)

2-amino-5-iodo-benzoic acid (263 mg, 1.0 mmol, 1 eq), phenylboronic acid (122 mg, 1.0 mmol, 1 eq), potassium carbonate (276 mg, 2.0 mmol, 2 eq), and palladium 10% on activated charcoal (0.03 eq) were dissolved in water (6 mL). The mixture was heated at reflux for 4h and then filtrated through cotton. The filtrate was acidified with an aqueous solution of HCl (1M) until pH reached 6. The aqueous layer was then extracted with EtOAc. The organic layer was dried over MgSO₄, concentrated in vacuo to give 2-amino-5-phenyl-benzoic acid (Yield: 94%). The product was used in the next step without further purification. 2-amino-5-phenyl-benzoic acid (200 mg, 0.94 mmol, 1 eq), di-*tert*-butyl dicarbonate (409 mg, 1.8 mmol, 2 eq), DMAP (8 mg, 0.06 mmol, 0.065 eq) and TEA (131 μL, 0.94 mmol, 1 eq) were dissolved in MeCN (3 mL). The mixture was vortexed, heated at 40 °C under microwave irradiation for 15 min. The mixture was then filtrated through cotton. The filtrate was concentrated in

vacuo and the residue was purified by preparative HPLC to give 2-(tert-butoxycarbonylamino)-5-phenyl-benzoic acid. Yield: 4%. ¹H-NMR (DMSO-d₆): δ (ppm) 10.69 (s, NH), 8.38 (d, *J* = 8.9 Hz, 1H), 8.21 (d, *J* = 2.3 Hz, 1H), 7.89 (dd, *J* = 8.8 Hz, *J* = 2.3 Hz, 1H), 7.69 – 7.62 (m, 2H), 7.51 – 7.43 (m, 2H), 7.36 (tt, *J* = 7.4 Hz, *J* = 1.2 Hz, 1H), 1.50 (s, 9H). ¹³C-NMR (DMSO-d₆): δ (ppm) 170.0, 152.5, 141.2, 139.3, 133.5, 132.6, 129.5, 129.4, 127.8, 126.7, 119.1, 80.7, 28.4. HRMS (TOF, ES-) *m/z* [M-H]⁻ calculated for C₁₈H₁₈NO₄ 312.1236, found 312.1241.

4.1.4. General method for the synthesis of compounds **15**, **16** and **17**

The appropriate chloroformate (2 eq) was added dropwise in a mixture of 2-amino-5-iodo-benzoic acid (0.7 mmol, 1 eq) dissolved in anhydrous pyridine (3 mL). The reaction mixture was stirred at RT for 1h. The appropriate chloroformate (0-2 eq) was then added dropwise, the reaction mixture was stirred at RT for 1 h and then evaporated. An aqueous solution of HCl (1M) was added on the residue, and then the product was extracted with EtOAc. The organic layer was washed three times with an aqueous solution of HCl (1M), dried over MgSO₄ and concentrated in vacuo to give the desired product.

4.1.4.1. 5-iodo-2-(isobutoxycarbonylamino)benzoic acid (**15**)

Yield: 62%. ¹H-NMR (DMSO-d₆): δ (ppm) 13.94 (brs, OH), 10.66 (s, NH), 8.20 (d, *J* = 2.1 Hz, 1H), 8.07 (d, *J* = 8.9 Hz, 1H), 7.89 (dd, *J* = 8.9 Hz, *J* = 2.2 Hz, 1H), 3.90 (d, *J* = 6.7 Hz, 2H), 1.92 (septuplet, *J* = 6.7 Hz, 1H), 0.91 (d, *J* = 6.8 Hz, 6H). ¹³C-NMR (DMSO-d₆): δ (ppm) 168.8, 153.2, 142.8, 141.3, 139.5, 120.9, 118.2, 85.1, 71.2, 27.9, 19.3. HRMS (TOF, ES-) *m/z* [M-H]⁻ calculated for C₁₂H₁₃NO₄I 361.9889, found 361.9907.

4.1.4.2. 2-(allyloxycarbonylamino)-5-iodo-benzoic acid (**16**)

The residue was purified by preparative HPLC. Yield: 39%. ¹H-NMR (DMSO-d₆): δ (ppm) 10.71 (s, NH), 8.21 (d, *J* = 2.1 Hz, 1H), 8.07 (d, *J* = 8.8 Hz, 1H), 7.91 (dd, *J* = 8.9 Hz, *J* = 2.2 Hz, 1H), 6.07 – 5.89 (m, 1H), 5.35 (dq, *J* = 17.3 Hz, *J* = 1.7 Hz, 1H), 5.25 (dq, *J* = 10.3 Hz, *J* = 1.7 Hz, 1H), 4.63 (dt, *J* = 5.5 Hz, *J* = 1.4 Hz, 2H). ¹³C-NMR (DMSO-d₆): δ (ppm) 168.8, 152.8, 142.9, 141.1, 139.6, 133.2, 121.0, 118.6, 118.4, 85.4, 65.9. HRMS (TOF, ES-) *m/z* [M-H]⁻ calculated for C₁₁H₉NO₄I 345.9576, found 345.9597.

4.1.4.3. 2-(benzyloxycarbonylamino)-5-iodo-benzoic acid (**17**)

The residue was purified by preparative HPLC. Yield: 48%. ¹H-NMR (DMSO-d₆): δ (ppm) 14.04 (brs, OH), 10.73 (s, NH), 8.21 (d, *J* = 2.1 Hz, 1H), 8.10 (d, *J* = 8.8 Hz, 1H), 7.91 (dd, *J* = 8.9 Hz, *J* = 8.9 Hz, 1H), 7.46 – 7.30 (m, 5H), 5.18 (s, 2H). ¹³C-NMR (DMSO-d₆): δ (ppm) 168.8, 153.0, 142.9, 141.1, 139.6, 136.5, 129.0, 128.7, 121.0 (2C), 118.3, 85.4, 66.9. HRMS (TOF, ES-) *m/z* [M-H]⁻ calculated for C₁₅H₁₁NO₄I 395.9733, found 395.9752.

4.1.5. 2-(tert-butoxycarbonylamino)-5-iodo-benzoic acid (**18**)

To a solution of 2-(tert-butoxycarbonylamino)-5-iodo-benzoic acid (50 mg, 0.14 mmol, 1 eq) in anhydrous DMF (1 mL) was added cesium carbonate (157 mg, 0.48 mmol, 3.5 eq) followed by methyl iodide (20 μL, 0.32 mmol, 2.3 eq). The mixture was stirred at RT for 24h. LCMS analysis showed that the conversion was not complete. 150 mg of cesium carbonate (3.5 eq) and 20 μL of methyl iodide (2.3 eq) were added to the reaction mixture. The solution was stirred 24h at RT then filtered. The filtrate was poured in a tube and diluted in MeOH (4 mL). NaOH (40 mg, 1 mmol, 7.3 eq) and three drops of water were added and the mixture was stirred over the week-end at RT then evaporated. The residue was dissolved in water and the aqueous phase was washed twice with EtOAc. The aqueous phase was acidified to pH 4 with HCl then the product was extracted three times with EtOAc. The organic layers were assembled, washed once with brine, and then evaporated under reduced pressure to give 2-(tert-butoxycarbonylamino)-5-iodo-benzoic acid. Yield: 69%. ¹H-NMR (DMSO-d₆): δ (ppm) 13.21 (brs, OH), 8.03 (d, *J* = 1.8 Hz, 1H), 7.88 (dd, *J* = 8.4 Hz, *J* = 1.8 Hz, 1H), 7.14 (d, *J* = 8.4 Hz, 1H), 3.09 (s, 3H), 1.42 (s, 2H), 1.25 (s, 7H). ¹³C-NMR (DMSO-d₆): δ (ppm) 166.6, 153.5, 143.0, 141.5, 138.8, 132.2, 130.7, 91.8,

80.0, 37.6, 28.5, 28.1. HRMS (TOF, ES-) m/z [M-H]⁻ calculated for C₁₃H₁₅NO₄I 376.0046, found 376.0070.

4.1.6. Methyl 2-(tert-butoxycarbonylamino)-5-iodo-benzoate (19)

2-(tert-butoxycarbonylamino)-5-iodo-benzoic acid (182 mg, 0.5 mmol, 1 eq), dimethylsulfate (95 μ L, 1 mmol, 2 eq) and dipotassium carbonate (138 mg, 1 mmol, 2 eq) were dissolved in MeCN (2 mL). The mixture was stirred at RT for 2h. The solvent was evaporated in vacuo and the residue was solubilized in EtOAc. The organic layer was washed eight times with water and once with brine. The organic layer was dried over MgSO₄ and concentrated in vacuo to give methyl 2-(tert-butoxycarbonylamino)-5-iodo-benzoate. Yield: 28%. ¹H-NMR (DMSO-d₆): δ (ppm) 10.03 (s, NH), 8.15 (d, J = 2.0 Hz, 1H), 7.97 (d, J = 8.8 Hz, 1H), 7.90 (dd, J = 8.8 Hz, J = 2.1 Hz, 1H), 3.84 (s, 3H), 1.47 (s, 9H). ¹³C-NMR (DMSO-d₆): δ (ppm) 167.0, 152.3, 142.8; 140.8, 138.9, 121.6, 118.4, 85.3, 81.0, 53.2, 28.3. HRMS (TOF, ES-) not determined (non ionizable compound).

4.1.7. General method for the synthesis of compounds 20, 22 and 26

Step 1. SOCl₂ (1.1 mmol, 1.1 eq), 1H-benzotriazole (3.1 mmol, 3.1 eq) were mixed in DCM (2 mL) and then added dropwise to a solution of carboxylic acid (1 mmol, 1 eq) in DCM (2 mL). The reaction mixture was stirred overnight at RT and a precipitate appeared. The precipitate was filtered off and the filtrate was evaporated under reduced pressure. The product was used in the next without further purification.

Step 2. Benzotriazole derivative previously formed (0.5 mmol, 1 eq), 2-amino-5-iodo-benzoic acid (0.5 mmol, 1 eq) and DMAP (0.55 mmol, 1.1 eq) were dissolved in CHCl₃ (1 mL). The mixture was vortexed, heated at 80 °C under microwave irradiations for 30 min. The reaction mixture was diluted in EtOAc then washed twice with aqueous HCl (C = 1 M) and then once with brine. The organic layer was dried over MgSO₄ and concentrated in vacuo.

4.1.7.1. 2-benzamido-5-iodo-benzoic acid (20)

The residue was precipitated in a mixture of MeCN and MeOH (1:1), then filtered and washed with MeCN. Yield: 58%. ¹H-NMR (DMSO-d₆): δ (ppm) 14.10 (brs, OH), 12.09 (s, NH), 8.52 (d, J = 8.8 Hz, 1H), 8.30 (d, J = 2.4 Hz, 1H), 8.00 – 7.88 (m, 3H), 7.71 – 7.51 (m, 3H). ¹³C-NMR (DMSO-d₆): δ (ppm) 169.1, 165.2, 142.9, 141.1, 139.6, 134.7, 132.8, 129.5, 127.5, 122.5, 112.3, 86.7. HRMS (TOF, ES-) m/z [M-H]⁻ calculated for C₁₄H₉NO₃I 365.9627, found 365.9641.

4.1.7.2. 5-iodo-2-(3-phenylpropanoylamino)benzoic acid (22)

The residue was precipitated in a mixture of MeCN and MeOH (1:1), then filtered and washed with MeCN. Yield: 33%. ¹H-NMR (DMSO-d₆): δ (ppm) 13.94 (s, 1H), 11.04 (s, 1H), 8.28 (d, J = 8.8 Hz, 1H), 8.21 (d, J = 2.2 Hz, 1H), 7.90 (dd, J = 8.8 Hz, J = 2.2 Hz, 1H), 7.34 – 7.12 (m, 5H), 2.93 (t, J = 7.5 Hz, 2H), 2.71 (t, J = 7.5 Hz, 2H). ¹³C-NMR (DMSO-d₆): δ (ppm) 171.0, 168.6, 142.7, 141.1, 140.7, 139.4, 128.8, 128.7, 126.5, 122.7, 119.2, 86.2, 30.9. HRMS (TOF, ES-) m/z [M-H]⁻ calculated for C₁₆H₁₃NO₃I 393.9940, found 393.9962.

4.1.7.3. 2-(cyclopropanecarbonylamino)-5-iodo-benzoic acid (26)

The product was purified by reverse flash chromatography (MeOH/H₂O 20/80 to 80/20). Yield: 61%. ¹H-NMR (DMSO-d₆): δ (ppm) 11.28 (s, 1H), 8.26 (d, J = 8.9 Hz, 1H), 8.21 (d, J = 2.2 Hz, 1H), 7.87 (dd, J = 8.8, 2.3 Hz, 1H), 1.71 (quin, J = 6.1 Hz, 1H), 0.85 (d, J = 6.0 Hz, 4H). ¹³C-NMR (DMSO-d₆): δ (ppm) 171.8, 168.2, 142.1, 140.4, 138.9, 122.3, 118.6, 85.6, 16.0, 7.9. HRMS (TOF, ES-) m/z [M-H]⁻ calculated for C₁₁H₉NO₃I 329.9627, found 329.9652.

4.1.8. 5-iodo-2-[(2-phenylacetyl)amino]benzoic acid (21)

2-phenylacetyl chloride (185 μ L, 1.4 mmol, 2 eq) was added dropwise in a mixture of 2-amino-5-iodo-benzoic acid (184 mg, 0.7 mmol, 1 eq) dissolved in anhydrous pyridine (3 mL). The mixture was stirred

at RT for 1h, and then 2-phenylacetyl chloride (46 μ L, 0.35 mmol, 0.5 eq) was added dropwise. The reaction mixture was stirred at RT for 1h, then quenched with an aqueous solution of HCl (1M). The product was extracted with EtOAc and washed three times with an aqueous solution of HCl (1M). The organic layer was dried over $MgSO_4$ and concentrated in vacuo. The residue was purified by preparative HPLC to give 5-iodo-2-[(2-phenylacetyl)amino]benzoic acid. Yield: 64%. 1H -NMR (DMSO- d_6): δ (ppm) 13.90 (brs, OH), 11.08 (s, NH), 8.31 (d, $J = 8.8$ Hz, 1H), 8.19 (d, $J = 2.2$ Hz, 1H), 7.90 (dd, $J = 8.8$ Hz, $J = 2.2$ Hz, 1H), 7.41 - 7.23 (m, 5H), 3.76 (s, 2H). ^{13}C -NMR (DMSO- d_6): δ (ppm) 170.1, 168.5, 142.7, 140.8, 139.4, 135.1, 130.0, 129.1, 127.5, 122.5, 119.2, 86.4, 45.0. HRMS (TOF, ES-) m/z [M-H]- calculated for $C_{15}H_{11}NO_3I$ 379.9784, found 379.9794.

4.1.9. 5-iodo-2-(4-phenylbutanoylamino)benzoic acid (23)

4-phenylbutanoic acid (690 mg, 4.2 mmol, 3 eq) was dissolved in EtOAc dried over molecular sieves (15 mL), with PyBrop (1.96 g, 4.2 mmol, 3 eq) and DIEA (1.46 mL, 8.4 mmol, 6 eq). The solution was added to the HOBt resin (1-Hydroxybenzotriazole-6-sulfonamidomethyl polymer-bound, 1.4 mmol, 1 eq) and the resin was shaken for 3h at RT. After the first activation step the resin was washed 3 times with DMF. The second activation step was performed under the same conditions and the resin was washed 5 times with DMF then twice with DCM and dried. The polymer-bound activated ester (146 mg, 0.25 mmol, 1.25 eq) and 2-amino-5-iodo-benzoic acid (52 mg, 0.2 mmol, 1 eq) were dissolved in DMF dried over molecular sieves (1 mL). The mixture was stirred overnight at RT. The conversion was around 70%. The supernatant was separated from the resin by filtration. The polymeric beads were washed 3 times with DMF, the washing solutions were recovered and combined with the supernatant previously recovered. The solvent was evaporated in vacuo. The residue was purified by preparative HPLC to give 5-iodo-2-(4-phenylbutanoylamino)benzoic acid. Yield: 46%. 1H -NMR (DMSO- d_6): δ (ppm) 13.91 (brs, OH), 11.06 (s, NH), 8.30 (d, $J = 8.8$ Hz, 1H), 8.21 (d, $J = 2.2$ Hz, 1H), 7.90 (dd, $J = 8.8$ Hz, $J = 2.2$ Hz, 1H), 7.34 - 7.14 (m, 5H), 2.63 (t, $J = 7.5$ Hz, 2H), 2.40 (t, $J = 7.5$ Hz, 2H), 1.92 (quin, $J = 7.5$ Hz, 2H). ^{13}C -NMR (DMSO- d_6): δ (ppm) 171.6, 168.6, 142.6, 142.0, 140.8, 139.4, 128.8, 128.8, 126.3, 122.7, 119.4, 86.2, 37.3, 34.9, 27.0. HRMS (TOF, ES-) m/z [M-H]- calculated for $C_{17}H_{15}NO_3I$ 408.0097, found 408.0111.

4.1.10. General method for the synthesis of compounds **24**, **25**, **28-34**, **36** and **37**

Step 1. A 1 M solution of isopropyl chloroformate in toluene (1.5 eq) was added in anhydrous THF under argon. The appropriate carboxylic acid (1 eq) was dissolved in anhydrous THF ($C = 1.0$ M) with TEA (1.2 eq). This solution was added dropwise to the isopropyl chloroformate solution at 0 $^{\circ}C$. The mixture was allowed to warm to RT, stirred overnight and then evaporated under reduced pressure. $NaHCO_3$ sat. was added and the product was extracted twice with EtOAc. The organic layer was washed once with $NaHCO_3$ sat., once with brine, dried over $MgSO_4$ and then evaporated under reduced pressure. The yield is supposed to be quantitative, and the product was used in the next step without further purification.

Step 2. 2-amino-5-iodo-benzoic acid (1 eq) was dissolved in water ($C = 0.5$ M) with sodium carbonate (2 eq). This solution was cooled to 0 $^{\circ}C$. The previously formed anhydride (1.5 eq) dissolved in THF ($C = 0.8$ M) was added dropwise at 0 $^{\circ}C$ to this solution. The mixture was stirred at RT for 3 h or overnight. The solvent was then evaporated under reduced pressure. The residue was purified by reverse flash chromatography ($H_2O/MeOH$ 90/10 to 0/100 over 25 min) to give the desired product.

4.1.10.1. 2-(indane-2-carbonylamino)-5-iodo-benzoic acid (24)

Yield: 49%. 1H -NMR (DMSO- d_6): δ (ppm) 14.50 (s, 1H), 8.30 (d, $J = 8.7$ Hz, 1H), 8.27 (d, $J = 2.3$ Hz, 1H), 7.56 (dd, $J = 8.7$ Hz, $J = 2.40$ Hz, 1H), 7.25 - 7.17 (m, 2H), 7.16 - 7.10 (m, 2H) 3.3 (t, $J = 7.4$ Hz, 1H), 3.17 (d, $J = 7.5$ Hz, 4H). ^{13}C -NMR (DMSO- d_6): δ (ppm) 173.0, 168.8, 142.3, 141.0, 140.0, 138.6, 127.7, 126.8,

124.7, 121.1, 85.2, 47.1, 36.5. HRMS (TOF, ES-) m/z [M-H]⁻ calculated for C₁₇H₁₃NO₃I 405.9940, found 405.9965.

4.1.10.2. 5-iodo-2-(tetralin-2-carbonylamino)benzoic acid (25)

Yield: 42%. ¹H-NMR (DMSO-d₆): δ (ppm) 14.50 (s, 1H) 8.32 (d, J = 8.7 Hz, 1H), 8.26 (d, J = 2.3 Hz, 1H), 7.58 (dd, J = 8.7 Hz, J = 2.6 Hz, 1H), 7.12 - 7.06 (m, 4H), 3.00 - 2.91 (m, 2H), 2.86 - 2.77 (m, 2H), 2.22 - 2.07 (m, 1H), 1.90 - 1.71 (m, 1H) ¹³C-NMR (DMSO-d₆): δ (ppm) 173.6, 168.6, 141.0, 140.0, 138.6, 136.0, 135.7, 129.4, 129.0, 127.8, 126.1, 126.0, 121.2, 85.2, 43.2, 32.3, 28.6, 26.4. HRMS (TOF, ES-) m/z [M-H]⁻ calculated for C₁₈H₁₅NO₃I 420.0097, found 420.0116.

4.1.10.3. 2-[(4-chlorobenzoyl)amino]-5-iodo-benzoic acid (28)

Yield: 49%. ¹H-NMR (DMSO-d₆): δ (ppm) 12.09 (s, 1H), 8.45 (d, J = 8.9 Hz, 1H), 8.29 (d, J = 2.1 Hz, 1H), 7.98 (dd, J = 8.8 Hz, J = 2.2 Hz, 1H), 7.94 (d, J = 8.9 Hz, 2H), 7.67 (d, J = 8.8 Hz, 2H). ¹³C-NMR (DMSO-d₆): δ (ppm) 168.6, 163.7, 142.4, 140.4, 139.1, 137.2, 133.1, 129.1, 129.0, 122.3, 119.2, 86.6. HRMS (TOF, ES-) m/z [M-H]⁻ calculated for C₁₄H₈NO₃ClI 399.9237, found 399.9267.

4.1.10.4. 2-[(3,4-dichlorobenzoyl)amino]-5-iodo-benzoic acid (29)

Yield: 82%. ¹H-NMR (DMSO-d₆): δ (ppm) 8.42 (d, J = 8.7 Hz, 1H), 8.31 (d, J = 2.3 Hz, 1H), 8.14 (d, J = 2.1 Hz, 1H), 7.95 (dd, J = 8.5 Hz, J = 2.1 Hz, 1H), 7.83 (d, J = 8.5 Hz, 1H), 7.65 (dd, J = 8.7 Hz, J = 2.5 Hz, 1H). ¹³C-NMR (DMSO-d₆): δ (ppm) 168.3, 162.3, 140.8, 140.1, 138.9, 136.1, 134.9, 132.2, 131.6, 129.6, 128.0, 127.7, 121.2, 86.3. HRMS (TOF, ES-) m/z [M-H]⁻ calculated for C₁₄H₇NO₃Cl₂I 433.8848, found 433.8862.

4.1.10.5. 2-[(2,4-dichlorobenzoyl)amino]-5-iodo-benzoic acid (30)

Yield: 66%. ¹H-NMR (DMSO-d₆): δ (ppm) 8.36 (d, J = 8.6 Hz, 1H), 8.29 (d, J = 2.3 Hz, 1H), 7.74 (d, J = 1.95 Hz, 1H), 7.67-7.62 (m, 2H), 7.54 (dd, J = 8.23 Hz, J = 1.96 Hz, 1H). ¹³C-NMR (DMSO-d₆): δ (ppm) 168.6, 163.8, 140.6, 140.1, 139.0, 136.4, 135.5, 131.7, 130.6, 130.1, 128.2, 127.7, 121.2, 86.5. HRMS (TOF, ES-) m/z [M-H]⁻ calculated for C₁₄H₇NO₃Cl₂I 433.8848, found 433.8866.

4.1.10.6. 5-iodo-2-[(4-methylbenzoyl)amino]benzoic acid (31)

Yield: 14%. ¹H-NMR (DMSO-d₆): δ (ppm) 8.49 (d, J = 8.7 Hz, 1H), 8.31 (d, J = 2.3 Hz, 1H), 7.91 (d, J = 8.2 Hz, 2H), 7.62 (dd, J = 8.7 Hz, J = 2.4 Hz, 1H), 7.34 (d, J = 7.9 Hz, 2H), 2.38 (s, 3H). ¹³C-NMR (DMSO-d₆): δ (ppm) 168.4, 164.7, 142.0, 141.2, 140.1, 138.6, 132.9, 129.7, 128.1, 127.7, 121.2, 85.5, 21.5. HRMS (TOF, ES-) m/z [M-H]⁻ calculated for C₁₅H₁₁NO₃I 379.9784 found 379.9810.

4.1.10.7. 5-iodo-2-[[4-(trifluoromethyl)benzoyl]amino]benzoic acid (32)

Yield: 58%. ¹H-NMR (DMSO-d₆): δ (ppm) 8.46 (d, J = 8.7 Hz, 1H), 8.32 (d, J = 2.3 Hz, 1H), 8.18 (d, J = 8.2 Hz, 2H), 7.92 (d, J = 8.2 Hz, 2H), 7.66 (dd, J = 8.7 Hz, J = 2.3 Hz, 1H). ¹³C-NMR (DMSO-d₆): δ (ppm) 168.6, 163.4, 140.9, 140.1, 139.4, 139.1, 131.9 (q, J = 32 Hz), 128.5, 127.4, 126.2 (q, J = 4.1 Hz), 124.3 (q, J = 27.2 Hz), 121.4, 86.4. HRMS (TOF, ES-) m/z [M-H]⁻ calculated for C₁₅H₈NO₃F₃I 433.9501, found 433.9510.

4.1.10.8. 5-iodo-2-[[4-(trifluoromethoxy)benzoyl]amino]benzoic acid (33)

Yield: 37%. ¹H-NMR (DMSO-d₆): δ (ppm) 8.45 (d, J = 8.6 Hz, 1H), 8.34 (d, J = 2.4 Hz, 1H), 8.12 (d, J = 8.8 Hz, 2H), 7.66 (dd, J = 8.6 Hz, J = 2.4 Hz, 1H), 7.53 (d, J = 8.8, 2H) ¹³C-NMR (DMSO-d₆): δ (ppm) 168.6, 163.4, 151.0 (q, J = 1.7 Hz), 141.0, 140.1, 138.9, 134.9, 130.0, 127.9, 121.4, 121.2, 120.2 (q, J = 256 Hz), 86.1. HRMS (TOF, ES-) m/z [M-H]⁻ calculated for C₁₅H₈NO₄F₃I 449.9450, found 449.9467.

4.1.10.9. 2-[[4-chloro-3-(trifluoromethyl)benzoyl]amino]-5-iodo-benzoic acid (34)

Yield: 48%. ¹H-NMR (DMSO-d₆): δ (ppm) 8.45 (d, J = 8.7 Hz, 1H), 8.39 (d, J = 1.6 Hz, 2H), 8.26 (dd, J = 8.4 Hz, J = 1.5 Hz, 1H), 7.95 (d, J = 8.4 Hz, 1H), 7.69 (dd, J = 8.6 Hz, J = 2.1 Hz, 1H). ¹³C-NMR (DMSO-d₆): δ (ppm) 168.3, 162.1, 140.9, 140.3, 139.2, 135.0, 134.4, 133.0, 132.9, 129.8 (q, J = 272 Hz), 127.7, 126.9,

126.8, 124.9, 121.2, 86.5. HRMS (TOF, ES-) m/z [M-H]⁻ calculated for C₁₅H₇NO₃F₃Cl 467.9111, found 467.9113.

4.1.10.10. 2-[(6-chloropyridine-3-carbonyl)amino]-5-iodo-benzoic acid (36)

Yield: 69%. ¹H-NMR (DMSO-d₆): δ (ppm) 8.95 (d, *J* = 2.2 Hz, 1H), 8.42 (d, *J* = 8.7 Hz, 1H) 8.36 – 8.30 (m, 2H), 7.72 (d, *J* = 8.7 Hz, 1H), 7.66 (dd, *J* = 8.4 Hz, *J* = 2.3 Hz, 1H). ¹³C-NMR (DMSO-d₆): δ (ppm) 168.6, 162.0, 153.3, 149.4, 140.8, 140.1, 139.1, 138.8, 130.7, 127.7, 125.0, 121.3, 86.5. HRMS (TOF, ES-) m/z [M-H]⁻ calculated for C₁₃H₇N₂O₃Cl 400.9190, found 400.9217.

4.1.10.11. 2-[[[(E)-3-(4-chlorophenyl)prop-2-enoyl]amino]-5-iodo-benzoic acid (37)

Yield: 61%. ¹H-NMR (DMSO-d₆): δ (ppm) 8.40 (d, 1H, *J* = 8.7 Hz) 8.28 (d, 1H, *J* = 2.3 Hz) 7.72 (d, 2H, *J* = 8.5 Hz), 7.60 (dd, 1H, *J* = 8.7 Hz, *J* = 2.3 Hz), 7.54 (d, 1H, *J* = 15.7 Hz) 7.47 (d, 2H, *J* = 8.5 Hz), 6.67 (d, 1H, *J* = 15.7 Hz) ¹³C-NMR (DMSO-d₆): δ (ppm) 168.5, 163.6, 141.0, 140.1, 139.0, 138.7, 134.6, 134.1, 130.1, 129.4, 127.9, 124.8, 121.4, 85.8. HRMS (TOF, ES-) m/z [M-H]⁻ calculated for C₁₆H₁₁ClINO₃ 425.9394, found 425.9405.

4.1.11. General method for the synthesis of compounds 27 and 35

Step 1. To a solution of methyl 2-amino-5-iodo-benzoate (0.5 mmol, 1 eq) in anhydrous pyridine (3 mL) was added the appropriate acyl chloride (0.55 mmol, 1.1 eq) dropwise at 0 °C. The reaction mixture was stirred at RT for 2 h. Aqueous HCl (C = 1M) was added to the solution and the product was extracted twice with EtOAc. The organic layers were washed twice with aqueous HCl (C = 1 M), once with brine, dried over MgSO₄ and then concentrated in vacuo. The product was used in the next without further purification.

Step 2. Lithium hydroxide (1.5 mmol, 3 eq) dissolved in water (4 mL) was added dropwise to a solution of the methylbenzoate derivative previously formed (0.5 mmol, 1 eq) dissolved in THF (4 mL). The mixture was stirred at RT for 1 h. THF was then evaporated under reduced pressure.

4.1.11.1. 2-[(3-chlorobenzoyl)amino]-5-iodo-benzoic acid (27)

An aqueous solution of HCl (C = 1 M) was added and the product was extracted twice with EtOAc. The organic layer was then washed once with brine, dried over MgSO₄ and concentrated in vacuo. Yield: 60 %. ¹H-NMR (DMSO-d₆): δ (ppm) 14.14 (brs, OH), 12.07 (s, NH), 8.42 (d, *J* = 8.8 Hz, 1H), 8.28 (d, *J* = 2.1 Hz, 1H), 7.99 (dd, *J* = 8.8 Hz, *J* = 2.2 Hz, 1H), 7.93 (d, *J* = 1.7 Hz, 1H), 7.88 (d, *J* = 7.8 Hz, 1H), 7.73 (dd, *J* = 7.0, 1.8 Hz, 1H), 7.63 (t, *J* = 7.8 Hz, 1H). ¹³C-NMR (DMSO-d₆): δ (ppm) 169.1, 163.7, 142.9, 140.6, 139.6, 136.8, 134.2, 132.6, 131.5, 127.4, 126.2, 122.8, 119.9, 87.2. HRMS (TOF, ES-) m/z [M-H]⁻ calculated for C₁₄H₈NO₃Cl 399.9237, found 399.9260.

4.1.11.2. 5-iodo-2-(pyridine-4-carbonylamino)benzoic acid (35)

An aqueous solution of HCl (C = 1 M) was added and the product precipitated. The solid was filtered, washed with a 1:1 mixture of diethyl ether and cyclohexane (3 x 1 mL), and then dried. Yield: 66%. ¹H-NMR (DMSO-d₆): δ (ppm) 8.80 (dd, *J* = 4.5 Hz, *J* = 1.5 Hz, 2H), 8.45 (d, *J* = 8.6 Hz, 1H), 8.34 (d, *J* = 2.3 Hz, 1H), 7.89 (dd, *J* = 4.5, 1.6 Hz, 2H), 7.66 (dd, *J* = 8.6, 2.2 Hz, 1H). ¹³C-NMR (DMSO-d₆): δ (ppm) 167.9, 162.9, 151.1, 142.6, 140.7, 140.1, 138.8, 128.3, 121.5, 121.3, 86.6. HRMS (TOF, ES-) m/z [M-H]⁻ calculated for C₁₃H₈N₂O₃I 366.9580, found 366.9603.

4.2 Biology

4.2.1. MabA expression and purification

E. coli BL21 (DE3) transformed with pET28a_MabA-His₆ were induced with 0.5 mM IPTG at an OD of 0.6 for 4 hours at 37 °C. The bacteria were harvested by centrifugation and resuspended in lysis buffer Tris 50 mM pH7.5, NaCl 300 mM, 10 mM imidazole, supplemented with DNase and Compete EDTA-free protease inhibitor (Roche). The bacteria were lysed by two passages on French press. MabA-His₆

was purified on Ni²⁺-affinity column (His-trap, GE Healthcare), eluted in lysis buffer supplemented with 250 mM imidazole and dialysed against Tris 50 mM pH7.5, NaCl 300 mM. Glycerol at 10% was added to the protein for storage at -80 °C.

4.2.2. MabA enzymatic assay

NADPH, AcAcCoA and BCoA were purchased from Sigma Aldrich.

4.2.2.1. Screening assay

Screening was performed on EquipEx Imaginex Biomed platform at the Pasteur Institute of Lille. 200 nL of each compound at 100 mM in DMSO were transferred into black 384-well low-binding plates (Corning 3575) using an Echo 550 liquid Handler (Labcyte). 3.8 µL of Hepes buffer (100 mM pH 7) and 6 µL of MabA (1.33 µM in Hepes buffer) were added using a Bravo Automated Liquid Handler (Agilent). Plates were incubated for 10 or 30 minutes at 23 °C. The enzymatic reaction was started by adding 10 µL of a mixture of the substrate AcAcCoA and the cofactor NADPH (100 µM in Hepes buffer) using a Bravo Automated Liquid Handler. Plates were centrifuged 30 sec and then incubated for 15 minutes at 23 °C. The final concentrations were as follows: compound at 1 mM, MabA at 400 nM, AcAcCoA at 50 µM, NADPH at 50 µM, DMSO 1%. INH-NADP was used as a reference inhibitor (100% inhibition at 200 µM). The enzymatic reaction was stopped by adding 10 µL of a solution of trifluoroacetic acid in water at a final concentration of 1%, containing BCoA at a final concentration of 5 µM. Plates were sealed with a film and stored at -80 °C. Before analysis by LC-MS/MS, plates were centrifuged 4 min at 4000 rpm. Inhibition percentage of each compound was calculated using the mean values of the negative (1% DMSO) and positive controls (INH-NADP adduct at 200 µM). Z'-factors were calculated using the mean and standard deviation values (SD) of the negative and positive controls.[45] All the screening plates displayed a Z'-factor between 0.72 and 0.83.

$$\% Inh = 100 - \left(\frac{(x - Mean_{C+}) \times 100}{Mean_{C-} - Mean_{C+}} \right)$$

$$Z' = 1 - \frac{3(SD_{C+} + SD_{C-})}{|Mean_{C+} - Mean_{C-}|}$$

4.2.2.2. LC-MS/MS analysis

AcAcCoA, HBCoA and BCoA were detected by multiple-reaction monitoring (MRM) using a UPLC Acquity I-class coupled with a Xevo TQD mass spectrometer (Waters). Microplates were stored at 10 °C before analysis. AcAcCoA, HBCoA and BCoA were separated using an Acquity UPLC BEH C18 column (2.1 × 50 mm, 1.7 µm, Waters) at 40 °C and a flow rate of 0.6 mL/min. Mobile phase A: ammonium acetate 10 mM in water mQ. Mobile phase B: MeOH LC-MS grade. The gradient started at 2% B, increased linearly to 14% B in 1'20 and then to 98% B in 5 sec, held isocratic at 98% B for 30 sec, and returned to initial conditions. The column was equilibrated with initial conditions for 1.0 min before each injection. Source parameters were set as follows: polarity ES+, capillary 1200 V, desolvation temperature 600 °C, cone voltage 46 V, source temperature 150 °C, cone gas flow 50 L/h, desolvation gas flow 1200 L/h. Transitions monitored were as follows: AcAcCoA 852.1 - 342.5 (collision energy: 38 eV), HBCoA 854.1 - 347.2 (collision energy: 36 eV), BCoA 838.1 - 331.2 (collision energy: 34 eV). MassLynx software was used for mass spectrometry data acquisition and TargetLynx software was used for analysis (Waters). The relative amount of HBCoA in each well was determined by dividing the peak area of HBCoA by the peak area of BCoA used as an internal standard.

4.2.2.3. Preparation of INH-NADP adduct

The reference inhibitor used in this assay is the adduct of isoniazid (INH) with NADP⁺ which can be formed *in situ* using a solution of [Mn^{III}(H₂P₂O₇)₃]Na₃ (Mn₃PyrPh) at 5.5 mM prepared as described in the literature.[38] A solution of INH-NADP adduct (INH 2 mM, NADP⁺ 2 mM, Mn₃PyrPh 4 mM) was prepared by mixing 200 μL of INH (20 mM in HEPES buffer), 200 μL of NADP⁺ (20 mM in HEPES buffer), 1450 μL of Mn₃PyrPh (5.5 mM) and 150 μL of HEPES buffer. The solution was incubated at 22 °C for at least 20 min.

4.2.2.4. Dose-response experiments

Inhibition percentages of compounds at different concentrations were obtained using the protocol described for screening. Compounds at 100 mM in DMSO were transferred into black 384-well low-binding plates (Corning 3575) using an Echo 550 liquid Handler (Labcyte). Compounds were tested at 8 concentrations using 3-fold serial dilutions from 1 mM to 0.46 μM. DMSO volume was compensated so that the concentrations across all wells were equal to 1%. INH-NADP was used as a reference inhibitor (100% inhibition at 200 μM). 3.8 μL of HEPES buffer (100 mM pH 7) and 6 μL of MabA (1.33 μM in HEPES buffer) were added manually using a 16-channel VIAFLO II electronic pipette (Integra Biosciences). Compounds were incubated with MabA for 30 minutes at 22 °C before the enzymatic reaction was started by adding manually 10 μL of a mixture of the substrate AcAcCoA and the cofactor NADPH (100 μM in HEPES buffer). The final concentrations were as follows: MabA at 400 nM, AcAcCoA at 50 μM, NADPH at 50 μM. Plates were incubated for 15 minutes at 22 °C. The enzymatic reaction was stopped by adding manually 10 μL of a solution of trifluoroacetic acid in water at a final concentration of 1%, containing BCoA at a final concentration of 5 μM. Dose-response curves were analysed with GraphPad Prism using a nonlinear regression analysis. Reported IC₅₀ values are the average of at least two experiments.

4.2.2.5. Competition experiment

Inhibition percentages of compound **1** and INH-NADP adduct were obtained using the protocol described for dose-response experiments and two different NADPH concentrations (50 and 500 μM). Compound **1** was tested at 8 concentrations using 3-fold serial dilutions from 1 mM to 0.46 μM. INH-NADP adduct was tested at 8 concentrations using 3-fold serial dilutions from 200 μM to 0.09 μM.

4.2.3. ¹⁹F-NMR assay

The ¹⁹F NMR measurements were done at 298 K using 3 mm tubes (160 μL samples) on a Bruker 600 MHz Avance III HD spectrometer equipped with a CP-QCI-F cryoprobe with optimized ¹⁹Fluorine detection. The ¹⁹F NMR reference spectra were acquired on 160 μL samples containing a compound (**32**, **33** or **34**) at 100 μM, in the NMR buffer [50 mM Tris-Cl pH 7.5; 250 mM NaCl; 1% DMSO-d₆; 5% D₂O]. Then, ¹⁹F NMR spectra of the compounds were acquired in the presence of MabA at 20 μM in the same NMR buffer. Experiments have been acquired with the following parameters: TD = 8192 points; NS = 512 scans; relaxation delay D1 = 2 seconds; carrier frequency O1P = -65.0 ppm; spectral window sw = 20 ppm; and with ¹⁹F decoupling. The acquisition time was about 22 minutes per sample. NMR data have been processed with Bruker Topspin 4.06.

4.2.4. *M. tuberculosis* assay

Compounds dissolved in DMSO at 100 mM were transferred to a 384-well low-volume polypropylene plate (Corning, no. 3672) and used to prepare assay plates. Compounds were tested from 300 μM to

15 nM. Ten 3-fold serial dilutions of compounds were performed into black Greiner 384-well clear bottom polystyrene plates (Greiner, no. 781091) using an Echo 550 liquid Handler (Labcyte). DMSO volume was compensated so that the concentrations across all wells were equal to 0.3%. Two independent replicates were made for each setting. On the day of the experiment, 50 μ L of a culture of *M. tuberculosis*-GFP H37Rv (grown in 7H9, with 0.2% glycerol and 0.05% Tween80 and then diluted to an OD_{600nm} = 0.02) was transferred to each assay plate and incubated at 37 °C for 5 days. The fluorescence intensity was measured at Ex/Em = 485/535 nm using a Victor Multilabel Plate Reader (PerkinElmer). The following reference compounds were used as positive control in this assay: rifampicine (MIC = 4 ng/mL), isoniazid (MIC = 125 ng/mL) and ethionamide (MIC = 2 μ g/mL).

4.3. Physico-chemical properties

These experiments were analyzed using a UPLC Acquity I-class coupled with a Xevo TQD mass spectrometer (Waters) under MRM detection. Source parameters were set as follows: polarity ES-, capillary 0.5 kV, desolvation temperature 600 °C, cone voltage 42 V, source temperature 150 °C, cone gaz flow 50 L/h, desolvation gaz flow 1200 L/h. Transitions monitored were as follows: 433.8 - 389.9 (collision energy 20 eV).

4.3.1. LogD

5 μ L of a 10 mM solution of compound in DMSO was diluted in 245 μ L of a 1/1 octanol/PBS mixture at pH 7.4. The mixture was gently shaken for 2 h at room temperature. 10 μ L of each phase were diluted in 490 μ L of MeOH and analyzed by LC-MS/MS. Each compound was tested in triplicate. Log D was determined as the logarithm of the ratio of concentration of product in octanol and PBS, determined by mass signals.

4.3.2. Solubility

5 μ L of a 10 mM of compound solution in DMSO was diluted either in 245 μ L of PBS pH 7.4 or in 245 μ L of MeOH in triplicate. The tubes were gently shaken 24 h at room temperature, then centrifuged for 5 min at 4000 rpm. The mixtures were filtered over 0.45 μ m filters (Millex-LH Millipore). 10 μ L of each solution were diluted in 490 μ L of MeOH and analyzed by LC-MS/MS. The solubility was determined by the ratio of mass signal areas PBS/MeOH.

Acknowledgements

We thank Eva Bannerman for technical assistance. This work was supported by Feder (12001407 (D-AL) Equipex Imaginex BioMed), l'Agence Nationale de la Recherche (ANR) France (2FightTB, ANR-13-JSV5-0010-01), Institut National de la Santé et de la Recherche Médicale, Centre National de la Recherche Scientifique, Université de Lille, Institut Pasteur de Lille, Région Hauts-de-France. The NMR facilities were funded by the Région Hauts-de-France, CNRS, Institut Pasteur de Lille, European Community (FEDER), Ministère de l'Enseignement supérieur, de la Recherche et de l'Innovation (MESRI) and Lille University. René Wintjens is a Research Associate at the Belgian National Fund for Scientific Research (FRS-FNRS).

Abbreviations

AcAcCoA, acetoacetyl-CoA; ACP, acyl carrier protein; anh, anhydrous; BCoA, butyryl-CoA; FAS, fatty-acid synthase; Boc₂O, di-*tert*-butyldicarbonate; DCM, dichloromethane; DMAP, *N,N*-Dimethylpyridin-4-amine; DMF, dimethylformamide; DMSO, dimethylsulfoxide; DRC, dose-response curve; EtOAc, ethyl acetate; HBCoA, hydroxybutyryl-CoA; INH, isoniazid; MeCN, acetonitrile; MDR, multidrug-

resistant; MeOH, methanol; *M.tb*, *Mycobacterium tuberculosis*; RT, room temperature; SAR, structure-activity relationships; TB, tuberculosis; TEA, triethylamine.

References

- [1] F. Wang, R. Langley, G. Gulten, L.G. Dover, G.S. Besra, W.R. Jacobs, J.C. Sacchettini, Mechanism of thioamide drug action against tuberculosis and leprosy, *J. Exp. Med.* 204 (2007) 73–78. doi:10.1084/jem.20062100.
- [2] World Health Organization, Global tuberculosis report 2019, 2019. https://www.who.int/tb/publications/global_report/en/.
- [3] A. Zumla, P. Nahid, S.T. Cole, Advances in the development of new tuberculosis drugs and treatment regimens, *Nat. Rev. Drug Discov.* 12 (2013) 388–404. doi:10.1038/nrd4001.
- [4] B. Villemagne, C. Crauste, M. Flipo, A.R. Baulard, B. Déprez, N. Willand, Tuberculosis: The drug development pipeline at a glance, *Eur. J. Med. Chem.* 51 (2012) 1–16. doi:10.1016/J.EJMECH.2012.02.033.
- [5] E. Cox, K. Laessig, FDA Approval of Bedaquiline — The Benefit–Risk Balance for Drug-Resistant Tuberculosis, *N. Engl. J. Med.* 371 (2014) 689–691. doi:10.1056/NEJMp1314385.
- [6] N.J. Ryan, J.H. Lo, Delamanid: First Global Approval, *Drugs.* 74 (2014) 1041–1045. doi:10.1007/s40265-014-0241-5.
- [7] S.J. Keam, Pretomanid: First Approval, *Drugs.* 79 (2019) 1797–1803. doi:10.1007/s40265-019-01207-9.
- [8] M. Jankute, J.A.G. Cox, J. Harrison, G.S. Besra, Assembly of the Mycobacterial Cell Wall, *Annu. Rev. Microbiol.* 69 (2015) 405–423. doi:10.1146/annurev-micro-091014-104121.
- [9] K.J. Kieser, E.J. Rubin, How sisters grow apart: mycobacterial growth and division, *Nat. Rev. Microbiol.* 12 (2014) 550–562. doi:10.1038/nrmicro3299.
- [10] J. Liu, C.E. Barry, G.S. Besra, H. Nikaido, Mycolic acid structure determines the fluidity of the mycobacterial cell wall., *J. Biol. Chem.* 271 (1996) 29545–29551. doi:10.1074/jbc.271.47.29545.
- [11] H. Marrakchi, M.-A. Lanéelle, M. Daffé, Mycolic Acids: Structures, Biosynthesis, and Beyond, *Chem. Biol.* 21 (2014) 67–85. doi:10.1016/J.CHEMBIOL.2013.11.011.
- [12] E. Schweizer, J. Hofmann, Microbial type I fatty acid synthases (FAS): major players in a network of cellular FAS systems., *Microbiol. Mol. Biol. Rev.* 68 (2004) 501–517. doi:10.1128/MMBR.68.3.501-517.2004.
- [13] N. Elad, S. Baron, Y. Peleg, S. Albeck, J. Grunwald, G. Raviv, Z. Shakked, O. Zimhony, R. Diskin, Structure of Type-I Mycobacterium tuberculosis fatty acid synthase at 3.3 Å resolution, *Nat. Commun.* 9 (2018) 3886. doi:10.1038/s41467-018-06440-6.
- [14] A. Bhatt, V. Molle, G.S. Besra, W.R. Jacobs, L. Kremer, The Mycobacterium tuberculosis FAS-II condensing enzymes: Their role in mycolic acid biosynthesis, acid-fastness, pathogenesis and in future drug development, *Mol. Microbiol.* 64 (2007) 1442–1454. doi:10.1111/j.1365-2958.2007.05761.x.
- [15] C. Vilchèze, H.R. Morbidoni, T.R. Weisbrod, H. Iwamoto, M. Kuo, J.C. Sacchettini, W.R. Jacobs, Inactivation of the inhA-encoded fatty acid synthase II (FASII) enoyl-acyl carrier protein reductase induces accumulation of the FAS I end products and cell lysis of Mycobacterium smegmatis., *J. Bacteriol.* 182 (2000) 4059–4067. doi:10.1128/jb.182.14.4059-4067.2000.
- [16] T. Parish, G. Roberts, F. Laval, M. Schaeffer, M. Daffé, K. Duncan, Functional complementation of the essential gene fabG1 of Mycobacterium tuberculosis by Mycobacterium smegmatis fabG but not Escherichia coli fabG, *J. Bacteriol.* 189 (2007) 3721–3728. doi:10.1128/JB.01740-06.
- [17] A.K. Brown, A. Bhatt, A. Singh, E. Saparia, A.F. Evans, G.S. Besra, Identification of the dehydratase component of the mycobacterial mycolic acid-synthesizing fatty acid synthase-II complex, *Microbiology.* 153 (2007) 4166–4173. doi:10.1099/mic.0.2007/012419-0.
- [18] A. Bhatt, L. Kremer, A.Z. Dai, J.C. Sacchettini, W.R. Jacobs, Conditional depletion of KasA, a key enzyme of mycolic acid biosynthesis, leads to mycobacterial cell lysis., *J. Bacteriol.* 187 (2005) 7596–7606. doi:10.1128/JB.187.22.7596-7606.2005.
- [19] E.J. North, M. Jackson, R.E. Lee, New approaches to target the mycolic acid biosynthesis

- pathway for the development of tuberculosis therapeutics., *Curr. Pharm. Des.* 20 (2014) 4357–4378. doi:10.2174/1381612819666131118203641.
- [20] A. Banerjee, E. Dubnau, A. Quemard, V. Balasubramanian, K.S. Um, T. Wilson, D. Collins, G. de Lisle, W.R. Jacobs, *inhA*, a gene encoding a target for isoniazid and ethionamide in *Mycobacterium tuberculosis*, *Science* (80-). 263 (1994) 227–230. doi:10.1126/science.8284673.
- [21] L. Kremer, L.G. Dover, H.R. Morbidoni, C. Vilchèze, W.N. Maughan, A. Baulard, S.-C. Tu, N. Honoré, V. Deretic, J.C. Sacchettini, C. Locht, W.R. Jacobs, G.S. Besra, Inhibition of *InhA* activity, but not *KasA* activity, induces formation of a *KasA*-containing complex in mycobacteria., *J. Biol. Chem.* 278 (2003) 20547–20554. doi:10.1074/jbc.M302435200.
- [22] C. Vilchèze, F. Wang, M. Arai, M.H. Hazbón, R. Colangeli, L. Kremer, T.R. Weisbrod, D. Alland, J.C. Sacchettini, W.R. Jacobs, Transfer of a point mutation in *Mycobacterium tuberculosis inhA* resolves the target of isoniazid, *Nat. Med.* 12 (2006) 1027–1029. doi:10.1038/nm1466.
- [23] A.E. Grzegorzewicz, J. Korduláková, V. Jones, S.E.M. Born, J.M. Belardinelli, A. Vaquié, V.A.K.B. Gundi, J. Madacki, N. Slama, F. Laval, J. Vaubourgeix, R.M. Crew, B. Gicquel, M. Daffé, H.R. Morbidoni, P.J. Brennan, A. Quémard, M.R. McNeil, M. Jackson, A common mechanism of inhibition of the *Mycobacterium tuberculosis* mycolic acid biosynthetic pathway by isoxyl and thiacetazone., *J. Biol. Chem.* 287 (2012) 38434–38441. doi:10.1074/jbc.M112.400994.
- [24] L. Gannoun-Zaki, L. Alibaud, L. Kremer, Point mutations within the fatty acid synthase type II dehydratase components *HadA* or *HadC* contribute to isoxyl resistance in *Mycobacterium tuberculosis*., *Antimicrob. Agents Chemother.* 57 (2013) 629–632. doi:10.1128/AAC.01972-12.
- [25] J.M. Belardinelli, H.R. Morbidoni, Mutations in the essential FAS II β -hydroxyacyl ACP dehydratase complex confer resistance to thiacetazone in *Mycobacterium tuberculosis* and *Mycobacterium kansasii*, *Mol. Microbiol.* 86 (2012) 568–579. doi:10.1111/mmi.12005.
- [26] L. Kremer, J.D. Douglas, A.R. Baulard, C. Morehouse, M.R. Guy, D. Alland, L.G. Dover, J.H. Lakey, W.R. Jacobs, P.J. Brennan, D.E. Minnikin, G.S. Besra, Thiolactomycin and related analogues as novel anti-mycobacterial agents targeting *KasA* and *KasB* condensing enzymes in *Mycobacterium tuberculosis*., *J. Biol. Chem.* 275 (2000) 16857–16864. doi:10.1074/jbc.M000569200.
- [27] C.A. Machutta, G.R. Bommineni, S.R. Luckner, K. Kapilashrami, B. Ruzsicska, C. Simmerling, C. Kisker, P.J. Tonge, Slow onset inhibition of bacterial beta-ketoacyl-acyl carrier protein synthases by thiolactomycin., *J. Biol. Chem.* 285 (2010) 6161–6169. doi:10.1074/jbc.M109.077909.
- [28] K.A. Abrahams, C.W. Chung, S. Ghidelli-Disse, J. Rullas, M.J. Rebollo-López, S.S. Gurcha, J.A.G. Cox, A. Mendoza, E. Jiménez-Navarro, M.S. Martínez-Martínez, M. Neu, A. Shillings, P. Homes, A. Argyrou, R. Casanueva, N.J. Loman, P.J. Moynihan, J. Lelièvre, C. Selenski, M. Axtman, L. Kremer, M. Bantscheff, I. Angulo-Barturen, M.C. Izquierdo, N.C. Cammack, G. Drewes, L. Ballell, D. Barros, G.S. Besra, R.H. Bates, Identification of *KasA* as the cellular target of an anti-tubercular scaffold, *Nat. Commun.* 7 (2016). doi:10.1038/ncomms12581.
- [29] M. Cohen-Gonsaud, S. Ducasse, F. Hoh, D. Zerbib, G. Labesse, A. Quemard, Crystal structure of *MabA* from *Mycobacterium tuberculosis*, a reductase involved in long-chain fatty acid biosynthesis, *J. Mol. Biol.* 320 (2002) 249–261. doi:10.1016/S0022-2836(02)00463-1.
- [30] M. Cohen-Gonsaud, S. Ducasse-Cabanot, A. Quemard, G. Labesse, Ligand-induced fit in mycobacterial *MabA*: The sequence-specific C-terminus locks the conformational change, *Proteins Struct. Funct. Bioinforma.* 60 (2005) 392–400. doi:10.1002/prot.20494.
- [31] T. Küssau, M. Flipo, N. Van Wyk, A. Viljoen, V. Olieric, L. Kremer, M. Blaise, Structural rearrangements occurring upon cofactor binding in the *Mycobacterium smegmatis* β -ketoacyl-acyl carrier protein reductase *MabA*, *Acta Crystallogr. Sect. D Struct. Biol.* 74 (2018) 383–393. doi:10.1107/S2059798318002917.
- [32] A. Dessen, A. Quémard, J.S. Blanchard, W.R. Jacobs, J.C. Sacchettini, Crystal structure and function of the isoniazid target of *Mycobacterium tuberculosis*, *Science* (80-). 267 (1995) 1638–1641. doi:10.1126/science.7886450.

- [33] D.A. Rozwarski, C. Vilchèze, M. Sugantino, R. Bittman, J.C. Sacchettini, Crystal structure of the Mycobacterium tuberculosis enoyl-ACP reductase, InhA, in complex with NAD⁺ and a C16 fatty acyl substrate, *J. Biol. Chem.* 274 (1999) 15582–15589. doi:10.1074/jbc.274.22.15582.
- [34] S. Ducasse-Cabanot, M. Cohen-Gonsaud, H. Marrakchi, M. Nguyen, D. Zerbib, J. Bernadou, M. Daffé, G. Labesse, A. Quémard, In Vitro Inhibition of the Mycobacterium tuberculosis β -Ketoacyl-Acyl Carrier Protein Reductase MabA by Isoniazid, *Antimicrob. Agents Chemother.* 48 (2004) 242–249. doi:10.1128/AAC.48.1.242-249.2004.
- [35] H. Marrakchi, S. Ducasse, G. Labesse, H. Montrozier, E. Margeat, L. Emorine, X. Charpentier, M. Daffé, A. Quémard, MabA (FabG1), a Mycobacterium tuberculosis protein involved in the long-chain fatty acid elongation system FAS-II, *Microbiology.* 148 (2002) 951–960. doi:10.1099/00221287-148-4-951.
- [36] R.G. Silva, L.P.S. De Carvalho, J.S. Blanchard, D.S. Santos, L.A. Basso, Mycobacterium tuberculosis β -ketoacyl-acyl carrier protein (ACP) reductase: Kinetic and chemical mechanisms, *Biochemistry.* 45 (2006) 13064–13073. doi:10.1021/bi0611210.
- [37] R.A. Copeland, Mechanistic considerations in high-throughput screening, *Anal. Biochem.* 320 (2003) 1–12. doi:10.1016/S0003-2697(03)00346-4.
- [38] M. Nguyen, C. Claparols, J. Bernadou, B. Meunier, A Fast and Efficient Metal-Mediated Oxidation of Isoniazid and Identification of Isoniazid-NAD(H) Adducts, *ChemBioChem.* 2 (2001) 877–883. doi:10.1002/1439-7633(20011203)2:12<877::AID-CBIC877>3.0.CO;2-V.
- [39] S.L. Parikh, G. Xiao, P.J. Tonge, Inhibition of InhA, the enoyl reductase from Mycobacterium tuberculosis, by triclosan and isoniazid, *Biochemistry.* 39 (2000) 7645–7650. doi:10.1021/bi0008940.
- [40] R.C. Hartkoorn, F. Pojer, J.A. Read, H. Gingell, J. Neres, O.P. Horlacher, K.H. Altmann, S.T. Cole, Pyridomycin bridges the NADH- and substrate-binding pockets of the enoyl reductase InhA., *Nat. Chem. Biol.* 10 (2014) 96–98. doi:10.1038/nchembio.1405.
- [41] R.C. Hartkoorn, C. Sala, J. Neres, F. Pojer, S. Magnet, R. Mukherjee, S. Uplekar, S. Boy-Röttger, K.H. Altmann, S.T. Cole, Towards a new tuberculosis drug: Pyridomycin - nature's isoniazid, *EMBO Mol. Med.* 4 (2012) 1032–1042. doi:10.1002/emmm.201201689.
- [42] H. Prevet, M. Flipo, P. Roussel, B. Deprez, N. Willand, Microwave-assisted synthesis of functionalized spirohydantoin as 3-D privileged fragments for scouting the chemical space, *Tetrahedron Lett.* 57 (2016) 2888–2894. doi:10.1016/j.tetlet.2016.05.065.
- [43] N.C. Tran, H. Dhondt, M. Flipo, B. Deprez, N. Willand, Synthesis of functionalized 2-isoxazolines as three-dimensional fragments for fragment-based drug discovery, *Tetrahedron Lett.* 56 (2015) 4119–4123. doi:10.1016/j.tetlet.2015.05.035.
- [44] M. Congreve, R. Carr, C. Murray, H. Jhoti, A “Rule of Three” for fragment-based lead discovery?, *Drug Discov. Today.* 8 (2003) 876–877. doi:10.1016/S1359-6446(03)02831-9.
- [45] J.-H. Zhang, T.D.Y. Chung, K.R. Oldenburg, A Simple Statistical Parameter for Use in Evaluation and Validation of High Throughput Screening Assays, *J. Biomol. Screen.* 4 (1999) 67–73. doi:10.1177/108705719900400206.
- [46] R.A. Copeland, Evaluation of Enzyme Inhibitors in Drug Discovery: A Guide for Medicinal Chemists and Pharmacologists: Second Edition, Wiley, 2013. doi:10.1002/9781118540398.
- [47] T. Nittoli, K. Curran, S. Insaf, M. DiGrandi, M. Orlowski, R. Chopra, A. Agarwal, A.Y.M. Howe, A. Prashad, M.B. Floyd, B. Johnson, A. Sutherland, K. Wheless, B. Feld, J. O’Connell, T.S. Mansour, J. Bloom, Identification of anthranilic acid derivatives as a novel class of allosteric inhibitors of hepatitis C NS5B polymerase, *J. Med. Chem.* 50 (2007) 2108–2116. doi:10.1021/jm061428x.
- [48] S. Darakhshan, A.B. Pour, Tranilast: A review of its therapeutic applications, *Pharmacol. Res.* 91 (2015) 15–28. doi:10.1016/j.phrs.2014.10.009.
- [49] S. Silva, J.F. Shimizu, D.M. de Oliveira, L.R. de Assis, C. Bittar, M. Mottin, B.K. de P. Sousa, N.C. de M.R. Mesquita, L.O. Regasini, P. Rahal, G. Oliva, A.L. Perryman, S. Ekins, C.H. Andrade, L.R. Goulart, R. Sabino-Silva, A. Merits, M. Harris, A.C.G. Jardim, A diarylamine derived from anthranilic acid inhibits ZIKV replication, *Sci. Rep.* 9 (2019). doi:10.1038/s41598-019-54169-z.
- [50] A.S. El-Azab, A.A.M. Abdel-Aziz, S. Bua, A. Nocentini, N.A. AlSaif, A.A. Almehizia, M.M. Alanazi,

- M.M. Hefnawy, C.T. Supuran, New anthranilic acid-incorporating N-benzenesulfonamidophthalimides as potent inhibitors of carbonic anhydrases I, II, IX, and XII: Synthesis, in vitro testing, and in silico assessment, *Eur. J. Med. Chem.* 181 (2019) 111573. doi:10.1016/j.ejmech.2019.111573.
- [51] T.J. Sullivan, J.J. Truglio, M.E. Boyne, P. Novichenok, X. Zhang, C.F. Stratton, H.J. Li, T. Kaur, A. Amin, F. Johnson, R.A. Slayden, C. Kisker, P.J. Tonge, High affinity InhA inhibitors with activity against drug-resistant strains of *Mycobacterium tuberculosis*., *ACS Chem. Biol.* 1 (2006) 43–53. doi:10.1021/cb0500042.
- [52] X. He, A. Alian, P.R. Ortiz de Montellano, Inhibition of the *Mycobacterium tuberculosis* enoyl acyl carrier protein reductase InhA by arylamides, *Bioorganic Med. Chem.* 15 (2007) 6649–6658. doi:10.1016/j.bmc.2007.08.013.
- [53] S.R. Luckner, N. Liu, C.W. Am Ende, P.J. Tonge, C. Kisker, A slow, tight binding inhibitor of InhA, the enoyl-acyl carrier protein reductase from *Mycobacterium tuberculosis*, *J. Biol. Chem.* 285 (2010) 14330–14337. doi:10.1074/jbc.M109.090373.
- [54] M. Martínez-Hoyos, E. Perez-Herran, G. Gulten, L. Encinas, D. Álvarez-Gómez, E. Alvarez, S. Ferrer-Bazaga, A. García-Pérez, F. Ortega, I. Angulo-Barturen, J. Rullas-Trincado, D. Blanco Ruano, P. Torres, P. Castañeda, S. Huss, R. Fernández Menéndez, S. González del Valle, L. Ballell, D. Barros, S. Modha, N. Dhar, F. Signorino-Gelo, J.D. McKinney, J.F. García-Bustos, J.L. Lavandera, J.C. Sacchettini, M.S. Jimenez, N. Martín-Casabona, J. Castro-Pichel, A. Mendoza-Losana, Antitubercular drugs for an old target: GSK693 as a promising InhA direct inhibitor, *EBioMedicine.* 8 (2016) 291–301. doi:10.1016/j.ebiom.2016.05.006.
- [55] I.E. Pop, B.P. Déprez, A.L. Tartar, Versatile Acylation of N-Nucleophiles Using a New Polymer-Supported 1-Hydroxybenzotriazole Derivative, *J. Org. Chem.* 62 (1997) 2594–2603. doi:10.1021/jo961761g.
- [56] J.B. Jordan, L. Poppe, X. Xia, A.C. Cheng, Y. Sun, K. Michelsen, H. Eastwood, P.D. Schnier, T. Nixey, W. Zhong, Fragment based drug discovery: Practical implementation based on ¹⁹F NMR spectroscopy, *J. Med. Chem.* 55 (2012) 678–687. doi:10.1021/jm201441k.
- [57] J. Ribeiro, T. Diercks, J. Jiménez-Barbero, S. André, H.-J. Gabius, F. Cañada, Fluorinated Carbohydrates as Lectin Ligands: ¹⁹F-Based Direct STD Monitoring for Detection of Anomeric Selectivity, *Biomolecules.* 5 (2015) 3177–3192. doi:10.3390/biom5043177.
- [58] Y. Zhang, H. Zhang, Z. Sun, Susceptibility of *Mycobacterium tuberculosis* to weak acids, *J. Antimicrob. Chemother.* 52 (2003) 56–60. doi:10.1093/jac/dkg287.